BBA - Biomembranes 1867 (2025) 184431

Contents lists available at ScienceDirect

BBA - Biomembranes

journal homepage: www.elsevier.com/locate/bbamem

Research paper

Interaction of lensoside Aβ with lipids and proteins of HeLa cells

Justyna Kapral-Piotrowska [a,*], Agata Wawrzyniak [b], Jarosław Pawelec [c], Barbara Zarzyka [c], Roman Paduch [d], Jerzy Żuchowski [e], Adrianna Sławińska-Brych [f], Barbara Zdzisińska [d], Bartłomiej Pawlęga [g], Alicja Wójcik-Załuska [g], Ewa Baranowska-Wójcik [h], Joanna Jakubowicz-Gil [a], Wiesław I. Gruszecki [i], Bożena Pawlikowska-Pawlęga [a,c,**]

[a] Department of Functional Anatomy and Cytobiology, Institute of Biological Sciences, Maria Curie-Skłodowska University, Akademicka 19, 20-033 Lublin, Poland
[b] Department of Morphological Sciences, Institute of Medical Sciences, Medical College of Rzeszów University, Leszka Czarnego 4, 35-615 Rzeszów, Poland
[c] Electron Microscopy Laboratory, Maria Curie-Sklodowska University, Akademicka 19, 20-033 Lublin, Poland
[d] Department of Virology and Immunology, Institute of Biological Sciences, Maria Curie-Skłodowska University, Akademicka 19, 20-033 Lublin, Poland
[e] Department of Biochemistry, Institute of Soil Science and Plant Cultivation - State Research Institute, Czartoryskich 8, 24-100 Puławy, Poland
[f] Department of Cell Biology, Institute of Biological Sciences, Maria Curie-Skłodowska University, Akademicka 19, 20-033 Lublin, Poland
[g] Department of Clinical Physiotherapy, Faculty of Health Sciences, Medical University of Lublin, Poland
[h] Department of Biotechnology, Microbiology and Human Nutrition, University of Life Sciences, Skromna Street 8, 20-704 Lublin, Poland
[i] Department of Biophysics, Institute of Physics, Maria Curie-Skłodowska University, Pl. M. Curie-Skłodowskiej 1, 20-031 Lublin, Poland

ARTICLE INFO

Keywords:
Lensoside Aβ
Liposomes
HeLa cells
NMR
FTIR
SEM
TEM

ABSTRACT

Lensoside Aβ (LAβ) is a quercetin derivative isolated from the leaves and stems of the *Lens culinaris* cultivar Tina. Flavonoid-membrane interactions are crucial for their physiological and pharmacological activity. We have demonstrated the impact of LAβ on EYPC liposomes resembling the lipid phase of tumor cell membranes with the use of the ^{1}H NMR technique and have examined its activity on HeLa cells for the first time. To study the interactions of the tested compound with lipids and proteins at the molecular level, the FTIR technique was applied. To reveal changes in morphology and ultrastructure as well as examine its effect on apoptosis induction and cell viability, SEM, TEM, light, and fluorescence microscopy, flow cytometry analysis, LIVE/DEAD assays were employed. The ability of LAβ to induce oxidative stress was determined by staining with DHR123. The FTIR analyses indicated that LAβ interacts with the PO_{2-} groups in the polar head region. Moreover, a decrease in the relative protein concentration and changes in protein spectral profile in the amide I region were noted. Flavonoid reduced the viability of HeLa cells, which was correlated with the induction of apoptosis supported by SEM and TEM observations. Moreover, the addition of lensoside Aβ induced oxidative stress. These results confirm that lensoside Aβ may be used in novel therapeutic approaches for treating cervical cancer.

1. Introduction

Cervical cancer is a prevalent malignancy among women. It is the most common cause of cancer-related mortality worldwide. [1]. There are 530,000 new cases every year and more than half of these women die each year [2]. The main etiological agent of cervical cancer development is permanent infection with high-risk oncogenic human papillomavirus (HPV) [3]. Other factors that can trigger cervical cancer are young age of sexual initiation, multiple sexual partners, especially partners of "high risk", oral use of hormonal contraception, poor socioeconomic conditions, low level of personal hygiene, a numerous births and smoking [4]. To improve treatment efficacy and reduce the morbidity and mortality rate of cervical cancer, development of new, more effective, and novel therapeutic strategies is a priority [1].

* Corresponding author.
** Correspondence to: B.P. -Pawlęga, Electron Microscopy Laboratory, Maria Curie-Sklodowska University, Akademicka 19, 20-033 Lublin, Poland.
E-mail addresses: justyna.kapral-piotrowska@mail.umcs.pl (J. Kapral-Piotrowska), awawrzyniak@ur.edu.pl (A. Wawrzyniak), jaroslaw.pawelec@mail.umcs.pl (J. Pawelec), barbara.zarzyka@mail.umcs.pl (B. Zarzyka), rpaduch@poczta.umcs.lublin.pl (R. Paduch), jzuchowski@iung.pulawy.pl (J. Żuchowski), adrianna.slawinska-brych@mail.umcs.pl (A. Sławińska-Brych), barbara.zdzisinska@mail.umcs.pl (B. Zdzisińska), bartlomiej.pawlega@umlub.pl (B. Pawlęga), alicja.wojcik-zaluska@umlub.pl (A. Wójcik-Załuska), ewa.baranowska@up.lublin.pl (E. Baranowska-Wójcik), joanna.jakubowicz-gil@mail.umcs.pl (J. Jakubowicz-Gil), wieslaw.gruszecki@mail.umcs.pl (W.I. Gruszecki), bozena.pawlikowska-pawlega@mail.umcs.pl (B. Pawlikowska-Pawlęga).

https://doi.org/10.1016/j.bbamem.2025.184431
Received 29 July 2024; Received in revised form 11 June 2025; Accepted 18 June 2025
Available online 19 June 2025

Literature data show that a diet particularly rich in phytochemicals has a significant impact on some types of cancer [5,6]. Natural plant compounds, due to their safe action, low toxicity, and positive effect on the human body, have become the object of interest of many researchers. Understanding and describing the action mechanisms of new natural compounds should provide a novel insight into their use as natural drugs. One of the phytochemicals are flavonoids - secondary metabolites of plants, commonly present in vegetables, fruits, red wine, and black tea [7]. Flavonoids have been demonstrated to possess a wide range of biological and pharmacological activities, such as antioxidant, anticancer, antimicrobial, anti-inflammatory, and neuroprotective properties [8]. Due to inhibition of proliferation, modulation of signaling pathways, and induction of apoptosis, these phenolic compounds are promising strategies in cancer treatment [9]. The antioxidant effect of flavonoids is based on several mechanisms, including direct scavenging of reactive oxygen species (ROS), activation of antioxidant enzymes, metal chelating activity, and inhibition of free radical forming enzymes [10–12]. In contrast some flavonoids can acts as prooxidants. They cause apoptotic death of cancer cells by increasing ROS levels and modulate detoxifying enzymes [13]. Their prooxidant activity depends on concentration, structural characteristic, and culture conditions [14,15].

The edible lentil is an annual plant and belongs to the legume family. It is cultivated in many countries in North Africa, West, and South Asia, and Canada [16,17]. Contains a high level of active compound. Lentil seeds are a rich source of proteins (28 %), carbohydrates, minerals, and vitamin B [18,19]. Moreover, the seeds also contain phytosterols, saponins, phytic acids, lectins, polyphenols, and phytoestrogens [20–24]. These compounds prevent chronic diseases such as cancer, cardiovascular disease, obesity, and diabetes [25]. The flavonoids, especially those isolated from lentil seeds, are well known. These are mainly catechins and glycosides of quercetin, kaempferol, or luteolin [20–24]. However, currently little is known about flavonoids present in the underground parts of lentil [26–28]. One of these compounds present in the leaves and stems of edible lentils is lensoside Aβ (LAβ). This compound is a glycoside derivative of quercetin, which also contains caffeic acid in its structure. The interest in this compound stems from the fact that it is a new isolated compound. Furthermore, secondary metabolites from this part of the plant are not well studied [17]. Additionally, it interacts with membranes, the first targets for a drug [29].

The therapeutic effect of plant compounds, such as antioxidant or anticancer activity, is related to their incorporation into membranes and change in their fluidity [30–32]. Membranes of cancer cells, due to a high amount of unsaturated lipids and low cholesterol levels, are more liquid than normal cell membranes. The cell cycle and the initiation of apoptosis may be associated with changes in the fluidity of cancer cells. The increased membrane fluidity of tumor cells can be counteracted by membrane-stiffening compounds. There is data confirming that flavonoids prevent cancer cell membranes from fluidization. In addition, drugs can also trap free radicals or inhibit their diffusion through membrane fluidization or rigidity [33]. Our previous research showed that LAβ incorporates into model membranes formed with DPPC and creates hydrogen bonds with polar heads of lipids in the PO_{2-} group region and the C – O – P – O – C segment. ^{1}H NMR analysis revealed an ordering effect in both polar and non-polar region of the membrane. Furthermore, the parallel orientation of the tested compound with respect to the GUV membrane was confirmed by FLIM investigation [29].

Understanding the interaction of LAβ with the membrane may help to elucidate the molecular mechanisms of action and effects on cells that are essential for the treatment of many ailments. The objectives of this study were the investigation of the capacity of this flavonoid to interact with EYPC liposomes from egg yolk mimicking natural membranes and then examine its activity on protein and lipid components of HeLa cells. The present study is the first trial to explain such a mechanism of the novel flavonoid LAβ.

The application of the ^{1}H NMR technique allowed to determine the ability of the lensoside Aβ to o incorporate, interact, and alter the dynamic and structural attributes of EYPC liposomes. Fourier-transform infrared spectroscopy (FTIR) was carried out to reveal the effect of flavonoid on protein and lipid components of HeLa cells. The influence of LAβ on morphology, ultrastructure, morphometric parameters were determined with use of the scanning electron microscopy (SEM), the transmission electron microscopy (TEM) and light microscopy techniques. To address the issue of the impact of the examined compound on the initiation of apoptosis and the viability of the analyzed cells, a series of techniques were employed, including fluorescence microscopy, flow cytometry, NR assay, and LIVE/DEAD assay. Ultimately, the ROS level in tested cells was estimated by staining with DHR 123. The aforementioned techniques were applied to link the effect of lensoside Aβ on proteins and lipids of HeLa cells with apoptosis induction, viability, alterations in morphology and ultrastructure of cells. This may explain its mechanism of action on cancer cells, which is important for LAβ therapeutic activity.

2. Materials and methods

2.1. Chemicals

Lensoside Aβ was isolated from the aerial parts of *Lens culinaris* [17]. Flavonoid was dissolved in ethanol and was used for NMR experiments. The solution was stored in the dark. 1,2-diacyl-sn-glycero-3-phosphocholine from egg yolk (EYPC) was purchased from Sigma Chemical Co. Deuterium oxide (D_2O) was purchased from ARMAR Chemicals Co. (Switzerland). All other chemicals were of the best quality available.

2.2. Nuclear magnetic resonance (^{1}H NMR) analyses

Measurements were carried out according to the procedure described in the earlier paper [29]. Phospholipids (EYPC) and lensoside Aβ were dissolved in a chloroform/ethanol mixture (55:1 *v*/v) at the respective concentrations. The 1,2-diacyl-sn-glycero-3-phosphocholine concentration in the sample was $3{,}2{\cdot}10^{-2}$ M and of the flavonoid 3.2×10^{-4} M. First, samples were evaporated under a stream of nitrogen and then in a vacuum for 4 h. Next hydrated with D_2O samples were vigorously shaken for 1 h on a shaker at room temperature. To obtain a homogeneous lipid dispersion, lipid suspension was sonicated (8×3 s) with a sonicator (Sonics Vibra Cell™, Newtown, CT, USA) at 4 °C. 4 mM praseodymium trichloride ($PrCl_3$) was added before measurements.

^{1}H NMR spectra were performed on a Bruker Avance 300 NMR spectrometer using a 5-mm probe with pulsed field gradient capabilities. The ^{1}H NMR parameters were as follows: spectral window 10,333 Hz, digital resolution 0.1576 Hz, pulse width 6.5 μs, acquisition and delay time were 3.17 s and 1 s, respectively.

2.3. Cell culture

Human cervix carcinoma cells (HeLa, No 85060701) were obtained from the European Collection of Authenticated Cell Cultures (ECACC). Cells were grown in RPMI 1640 medium (GIBCO BRL) supplemented with 5 % FBS (GIBCO BRL) (*v*/v) and containing penicillin 100 U/mL, streptomycin 100 μg/mL and amphotericin B 0.25 μg/mL (Sigma). They were kept at 37 °C in a 5 % CO_2 humidified atmosphere. Experiments were conducted in 96-well plates, 25 cm^2 cell culture flasks, or in Leighton dishes for scanning electron microscopy and fluorescence microscopy. A stock solution of lensoside Aβ dissolved in dimethyl sulfoxide (DMSO) was applied. The final concentration of DMSO in final dilutions did not exceed 0.025 %.

2.4. LAβ treatment

A stock solution of lensoside Aβ dissolved in dimethyl sulfoxide (DMSO) was prepared and kept in the dark. In the study, LAβ at the final

concentrations of 5, 10, 15, 25, and 50 μg/mL was used. The HeLa cells were incubated with examined flavonol for 24 and 48 h.

2.5. FTIR spectroscopy of HeLa cells

The cells were seeded in petri dishes at a density of 1×10^5 cells/mL and were treated with lensoside Aβ for 24 and 48 h at the concentration of 15 μg/mL. Then the medium was removed, and monolayer cells were washed with PBS, carefully harvested using cell scrapers and suspended in PBS buffer supplemented with 5 % of D_2O. IR spectra of HeLa cells with and without examined flavonoid were recorded using the Fourier-transform infrared absorption spectrometer equipped with the attenuated total reflection set-up (ATR-FTIR). Measurements were carried out in accordance with the methodology described in the earlier article [34]. OPUS (Brucker, Germany) and Grams Al software from ThermoGalactic (USA) were used for spectral analyses.

2.6. Cell viability analysis by neutral red (NR) uptake assay and LIVE/DEAD kit

a) Neutral red uptake assay (NR)

NR assays were performed according to the procedure described in the previous paper [35]. Experiments were carried out in 96-well multiplates. After 24 and 48 h of incubation with LAβ at the doses of 5,10 15, 25 and 50 μg/mL, the medium was removed, 100 μL of NR were added to each well, and incubated for 3 h at 37 °C in standard conditions. Next, NR was removed from the plate, and each well was rinsed with fixative solution (200 μL) (0.5 % formalin in 1 % $CaCl_2$). Subsequently, 100 μL of solvent solution (1 % acetic acid in 50 % ethanol) was added to the wells and extracted for 20 min at room temperature. The absorbance was determined spectrophotometrically at wavelength $\lambda = 550$ nm using a plate reader (Emax; Molecular Devices Corp., Menlo Park, CA).

b) LIVE / DEAD cell viability test

The basis of this test is the different permeability of viable and damaged cells. In this test, SYTO 10 and DEAD red dyes were used. SYTO 10 is a green fluorescence dye, and it stains living cells, i.e. cells with an intact cell membrane. DEAD red is a red fluorescent dye and only stains cells with a damaged membrane [36]. 2 μL of SYTO 10 dye and 2 μL of DEAD red dye, which were dissolved in 1 mL of HBSS buffer, were used to prepare the staining mixture. Cells were incubated with the tested compound at the concentrations of 5, 10, 15, 25 and 50 μg/mL for 24 and 48 h. Next, cells were washed with HBSS buffer. Then 250 μL of the dye mixture solution was added and incubated for 15 min in the dark at room temperature. After that, cells were rinsed with HBSS buffer and fixed in 4 % glutaraldehyde for 1 h. Cells were washed again with fresh HBSS buffer. Observations were performed under a Nikon Labophot 2 fluorescence microscope at a wavelength of 490 nm. 1000 cells from randomly selected places were analyzed. The test was performed in triplicate.

2.7. Morphometric parameters of HeLa cells

For this study, HeLa cells were incubated with 15 μg/mL of examined flavonoid for 24 and 48 h. Then, the cells monolayer was washed with PBS, carefully scraped with a cell scraper, and fixed in 4 % glutaraldehyde for 1 h and post-fixed in 1 % osmium tetroxide for the next 1 h (at 4 °C). The samples were dehydrated in an increasing gradient of acetone (at room temperature) and embedded in LR White resin. The semi-thin sections were obtained with the RMC MT-XL microtome. The sections were stained with toluidine blue dye and analyzed under an Olympus BX40 light microscope equipped with a Soft Imaging System (SIS) ColorView III-u digital camera [37]. Morphometric parameters were measured and analyzed with a calibrated system, and the image was digitized using Soft Imaging System (SIS) Cell^D software. The cells selected for analysis were measured and counted by the program. Morphometric analysis was performed under 40 x magnification and included the area of the soma in μm^2, perimeter and diameter of the soma in μm.

2.8. Scanning electron microscopy (SEM) of HeLa cells

To determine changes in the morphology of HeLa cell surfaces after treatment with Laβ scanning electron microscopy was used. Cells were fixed in 4 % glutaraldehyde for 1 h and post-fixed in 1 % osmium tetroxide for a further 1,5 h. The procedure was performed at 4 °C. Samples were dehydrated in increasing concentrations of acetone (30–100 %) at room temperature, dried in a desiccator overnight, and coated with gold on an Emitech K550X sputter [37]. The samples were analyzed by using a TESCAN Vega 3 LMU microscope (Czech Republic).

2.9. Transmission electron microscopy (TEM) of HeLa cells

Transmission electron microscopy was used to study the cell ultrastructure. Cells, after treatment with LAβ were harvested using a cell scraper and rinsed with PBS buffer. Then cells were fixed for 1 h in 4 % glutaraldehyde and post-fixed in 1 % osmium tetroxide for 1,5 h at 4 °C. Next, samples were dehydrated with increasing acetone concentrations (30–100 %) at room temperature and embedded in LR White resin. After polymerization, obtained blocks were cut into ultrathin sections (65–75 nm) on a RMC MT-XL microtome (Tucson, Arizona, USA). The sections were collected on copper grids and contrasted with uranyl acetate and Reynolds' reagent. TEM measurements were carried out in the laboratory of Electron Microscopy of the Nencki Institute of Experimental Biology of the Polish Academy of Sciences in Warsaw with the application of the transmission electron microscope JEM 1400 (JEOL Co. Japan), equipped with a Roentgen microanalyzer (EDS INCA Energy TEM, Oxford Instruments, Great Britain) and a microscopic tomography system along with the CCD MORADA G2 (EMSIS GmbH, Germany) purchased from structural funds of UE within the project CZT BIM – "Equipping the biological and medical imaging laboratory."

2.10. Apoptosis and necrosis determination

a) fluorescent microscopy

To determine the level of apoptotic and necrotic cells staining with fluorochromes - propidium iodide and Hoechst 33342 dyes (Sigma) were used [37]. After 24 and 48 h of incubation with Laβ, 2.5 μL of the staining mixture was added to 1 mL of the medium and incubated at 37 °C for 5 min in darkness. The samples were analyzed under a fluorescence microscope, Nikon Labophot 2 fluorescence microscope equipped with a Canon Power Shot A 640 digital camera. Early apoptotic cells emitted bright blue fluorescence of nuclei, while pink fluorescence was characteristic for necrotic cells.

b) Flow cytometry

To quantify the number of apoptotic cells, an Annexin V- fluorescein isothiocyanate (FITC) apoptosis detection kit (BD Biosciences, BD Pharmingen™, USA) was used. Examined cells at a density of 6×10^5 cells/mL were cultured in 6-well plates. After the 24 h the growth medium was replaced with a medium containing lensoside Aβ. The analyses were performed in accordance with the methodology described in the earlier paper. Viable cells, early apoptotic cells, late apoptotic cells, and necrotic cells were analyzed using a FACS Calibur flow cytometer. The dye fluorescence was measured in the FL-1 and FL-3 channels.

2.11. Cells staining with dihydrorhodamine (DHR) 123

Staining with dihydrorhodamine 123 allows the detection of oxidative stress appearing in the cells. The DHR 123 dye has no charge and can diffuse passively across the membrane. In the cytoplasm of the cell, dihydrorhodamine is oxidized by reactive oxygen species (ROS) to cationic rhodamine 123, which in the mitochondria gives green fluorescence [38]. The generation of ROS was detected by

dihydrorhodamine 123 (DHR123) staining. After 24 and 48 h of incubation with the examined flavonoid, the cells were washed and resuspended in PBS buffer. Next, the dye DHR 123 was added to a final concentration of 0.5 μg/mL and incubated for 15 min at 37 °C. Observations were made using a Nikon Labophot 2 fluorescence microscope using a B-2 A filter.

3. Results

3.1. Modification of dynamics and structural attributes of EYPC model membranes by LAβ

The ^{1}H NMR technique was used to monitor the effect of LAβ with a model membrane formed with EYPC. Fig. 2 illustrates ^{1}H NMR spectra of EYPC liposomes without and with a supplement of 1 mol% flavonoid. (See Fig. 1.)

In the spectra there are visible bands that align with major molecular features of EYPC liposomes. Hydrophobic region of the membrane are represented by CH_3 and CH_2 groups (Fig. 2 c) while $N^+ - (CH_3)_3$ band is characteristic of the hydrophilic region of the membrane. Praseodymium chloride was added to the liposome suspension, which resulted in a split of the ^{1}H NMR band corresponding to the choline head region into two bands, one from the outer layer of the liposome membrane (N-$(CH_3)_3$ ^{out}) and the second from the inner layer of the liposome (N-$(CH_3)_3$ ^{in} (Fig. 2 b). The ratio of the area under the signals (I_{out} / I_{in}) assigned to the outer layer I_{out} to the inner layer I_{in} is proportional to the number of choline heads in the inner and outer layers of the membrane. A ratio of $I_{out}/I_{in} > 1$ is characteristic for small unilamellar liposomes, while for multilamellar liposomes it is lower than 1. The addition of LAβ decreased the value of the I_{out} / I_{in} ratio from 1.0624 for pure EYPC to 0.9395. Such an effect is most likely associated with the change in the physical attributes of the lipid bilayer that occurs as a result of flavonoid activity. Lensoside Aβ broadened the bands characteristic for CH_3 and CH_2 groups. It was observed that the value of the full width at half height (ν) exhibited an increase of 6.3 % and 14.4 %, respectively. The tested compound caused also the changes in the polar region of the phospholipids. In the presence of LAβ the value of ν parameters determined for N-$(CH_3)_3$ ^{in} and N-$(CH_3)_3^{out}$ groups increased by 7.8 % and 1.4 %, respectively. Moreover, examined flavonoid increased the splitting parameter of the resonance maximum characteristic for the choline head group (δ) from 0.1919 to 0.2002 ppm.

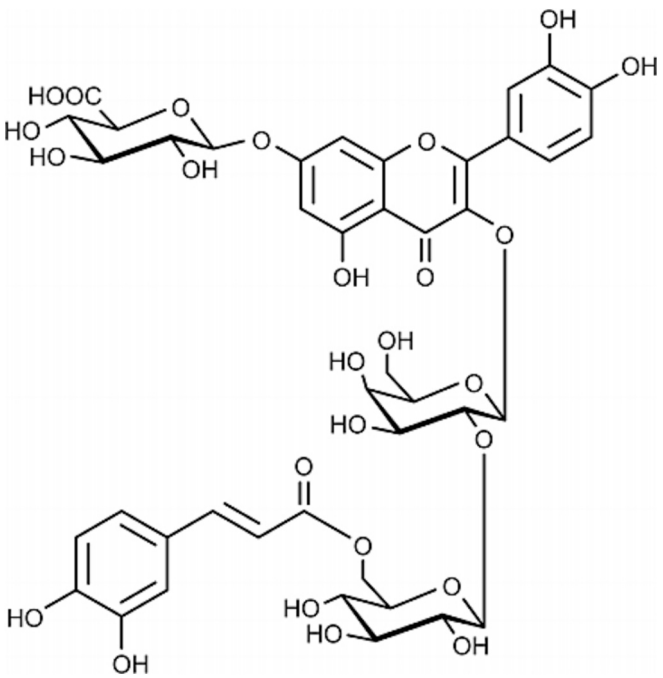

Fig. 1. Chemical structure of Lensoside Aβ (LAβ) molecule [17].

3.2. FTIR spectral analysis of HeLa cells after LAβ treatment

The FTIR spectroscopy was used to investigate the effects of lensoside Aβ on the HeLa cervical cancer line.

Representative FTIR spectra of control HeLa cells and cells treated for 24 and 48 h with the examined compound acquired in the region between 4000 and 900 cm^{-1} are shown in Figs. 3–6. Due to the low concentration of flavonoid relative to cellular components, its characteristic spectrum is not shown. All spectra were normalized over ~980 cm^{-1} peak characteristic for antisymmetric $N^+ - CH_3$ stretching vibrations.

In the region between 4000 and 970 cm^{-1}, absorption peaks characteristic of such molecules as proteins, lipids or nucleic acids are observed. The band centered at 2958 cm^{-1} and 2926 cm^{-1} (asymmetric C—H stretching vibrations of CH_3 and CH_2), 2872 cm^{-1} and 2854 cm^{-1} (symmetric C—H stretching vibrations of CH_3 and CH_2) are characteristics for lipids alkyl chains. Absorption at ~1741 cm^{-1} is attributed to ester C = O stretching of phospholipids. The signals between 1700 and 1600 cm^{-1} and 1580–1510 cm^{-1} correspond to the amide I and amide II of proteins. The region between 1300 and 900 cm^{-1} is usually assigned to phosphate groups related to nucleic acids (DNA, RNA) and phospholipids with dominant bands at ~1242 cm^{-1} (antisymmetric stretching of the PO_{2-} group) and 1086 cm^{-1} (symmetric stretching of the PO_{2-} group). The deformation vibration of the CH_2 group (known as scissoring vibration) is represented by the signals at ~1460 cm^{-1}. Bands with maxima at 1150 cm^{-1} and 1020–1025 cm^{-1} are characteristic for C—O bonds of glycogen and other carbohydrates. Spectral analysis revealed that exposure to LAβ has induced changes in the intensity of some bands.

Analysis of the spectra after a 24-h incubation with LAβ revealed the presence of a negative peak over 3287 cm^{-1}, which is characteristic of amide A. Furthermore, a reduction in intensity was observed in the bands representing the symmetric and antisymmetric stretching vibrations of the CH_2 i CH_3 groups of the alkyl chains (Fig. 3a). A positive band at 1747 cm^{-1} was noted in the difference spectrum (Fig. 3b). The Fig. 3c showed absorbance of infrared in the region between 1300 and 900 cm^{-1}. Our data revealed that the maximum characteristic for the symmetric stretching vibrations of the group - PO_{2-} (1082 cm^{-1}) is higher in the presence of lensoside Aβ than in HeLa control cells (Fig. 3c). This clearly indicates the interaction of flavonoid with this region by hydrogen bonds. At the same time, the absorption signals at 1237 cm^{-1} which are characteristic of the antisymmetric stretching vibrations of the - PO2- groups were weaker after LAβ treatment. In the difference spectrum, the appearance of the band with a maximum at 1155 cm^{-1} was found (Fig. 3c). The presence of lensoside Aβ in HeLa cells had significant effect on the amide I (1600–1700 cm^{-1}) region. The observation of a negative band in this region indicates a reduction in the relative protein content. To ascertain the molecular organization of the proteins, the amide I region was analyzed (see Fig. 4). Overall secondary protein structure affects the shape of the amide I band. In the 1700–1600 cm^{-1} area, peaks were attributed to antiparallel β-sheets (1675–1695 cm^{-1}), α-helices (1648–1660 cm^{-1}), β-sheets (1625–1640 cm^{-1}), unordered structures (1652–1660 cm^{-1}) and turns (1660–1685 cm^{-1}) [39]. Analysis of this region revealed that the addition of LAβ caused a significant increase in β-sheet structures (1638 cm^{-1}, 1623 cm^{-1}). Simultaneously, a clear decrease in turns (1665 cm^{-1}) and α-helices (1654 cm^{-1}) was revealed. This confirms that the tested compound causes partial protein aggregation (Fig. 4).

Treating HeLa cells with LAβ for 48 h resulted in changes to the IR absorption spectrum in the amide A (3300–3100 cm^{-1}), lipids (3000–2800 cm^{-1}) amide I (1700–1600 cm^{-1}) amide II (1580–1510 cm^{-1}) and 1200–900 cm^{-1} regions. Similarly to the 24-h incubation, a decrease in the 3300–3100 cm^{-1} region was noted. Fig. 5a demonstrates

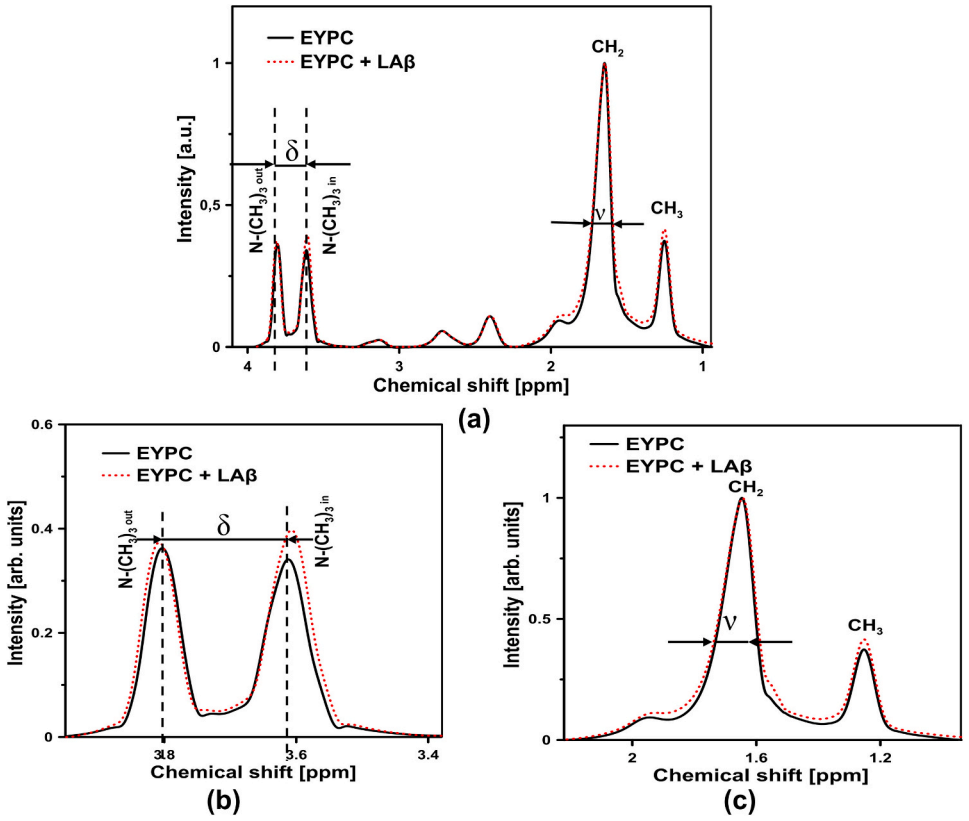

Fig. 2. ^{1}H NMR spectra of model membranes made of pure EYPC (continuous line) and EYPC with LAβ at 1 mol% (dashed line) (A), spectra representing the polar head region (B) spectra from the hydrophobic apolar region of the model mebrane (C). $PrCl_3$ was added to the samples prior to measurement. The graph illustrates the resonance line assignment and parameters employed in the spectral analysis. The following parameters were determined: the full width at half height (ν) and the splitting parameter of the resonance maximum corresponding to polar head groups (δ).

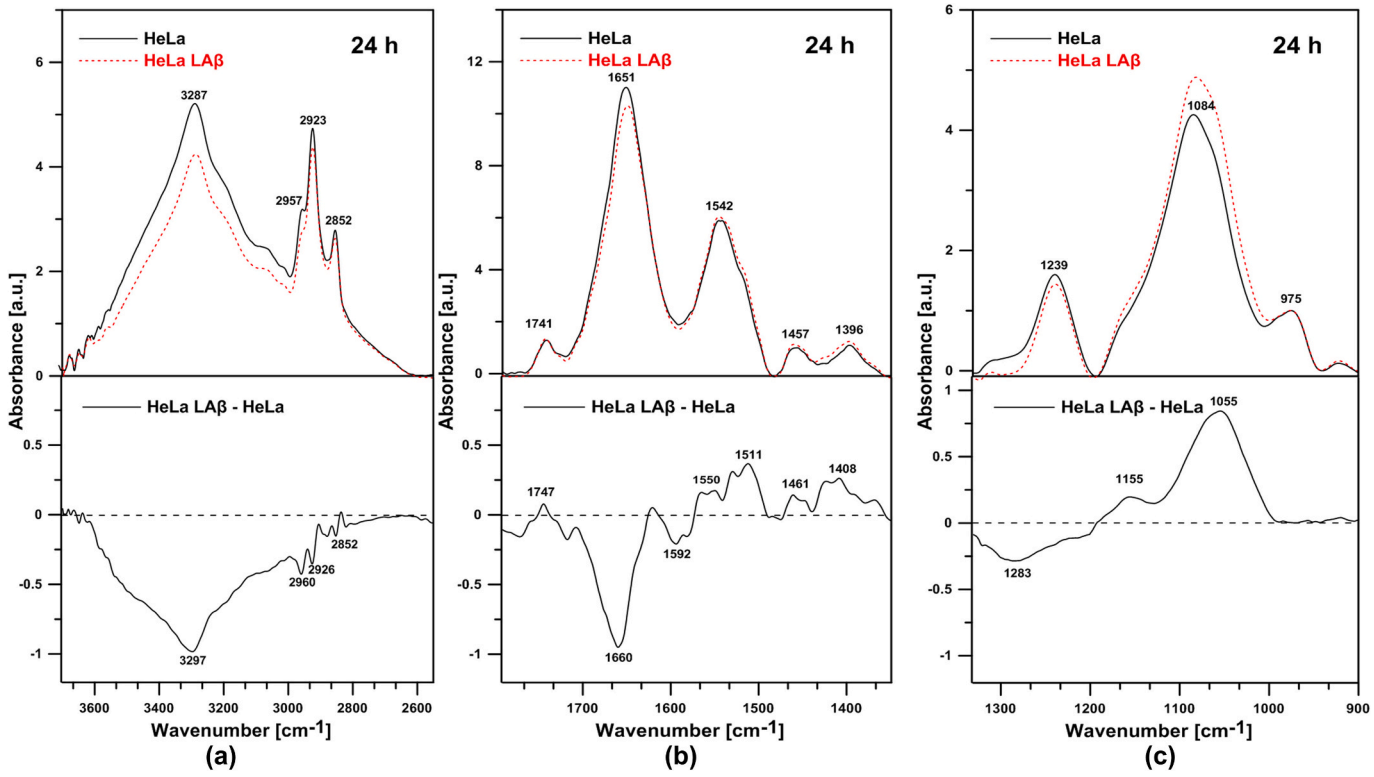

Fig. 3. Representative spectra of HeLa cells without and with the addition of lensoside Aβ of the a) 3800–2500 cm^{-1} b) 2000–1300 cm^{-1} c) 1300–900 cm^{-1} regions. At the bottom parts of graphs, difference spectra are shown.

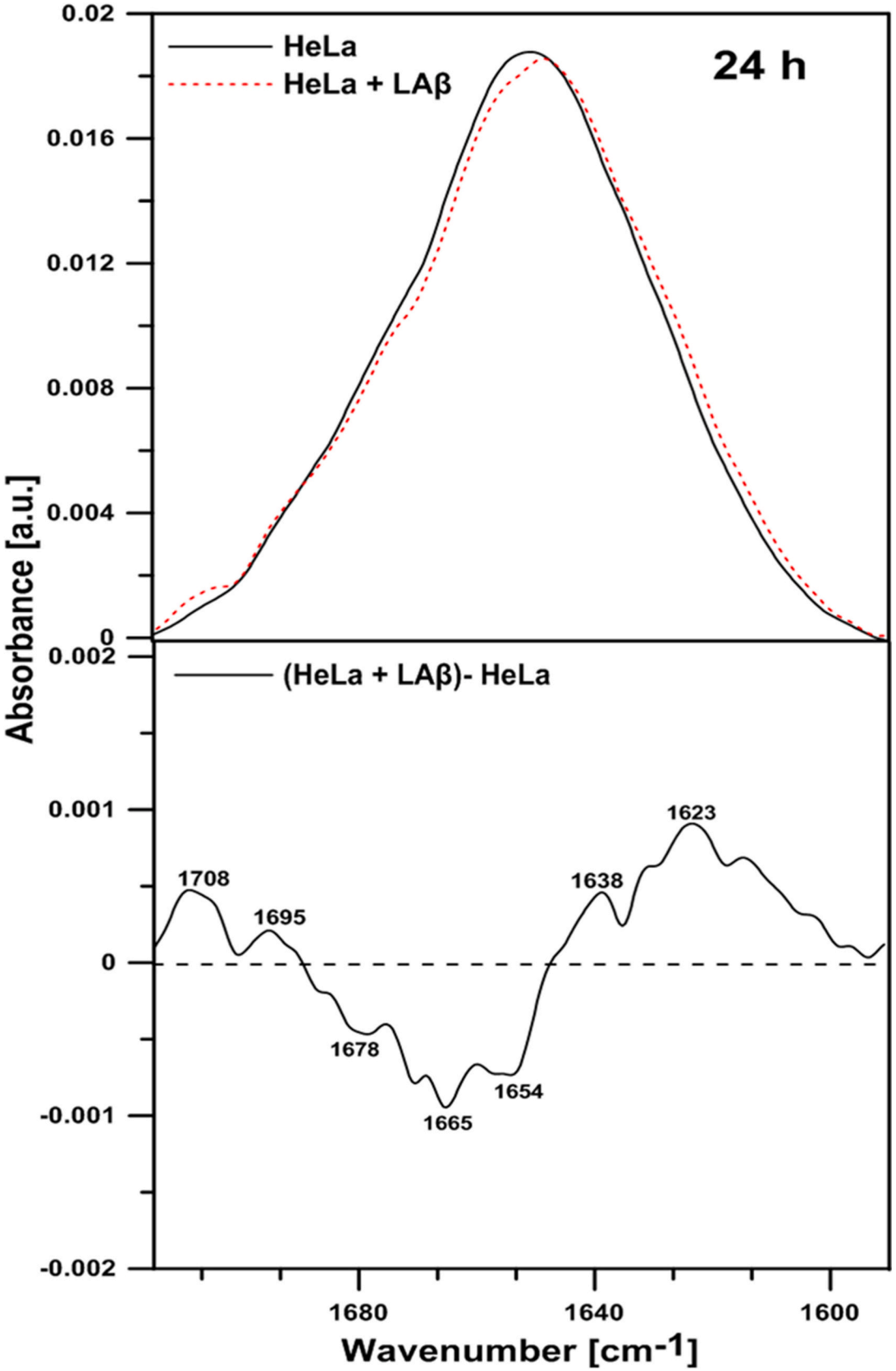

Fig. 4. The amide I region in HeLa control cells (upper part of the graph, black line) and treated with LAβ for 24 h (upper part of the graph, red, dashed line). The bottom part of the graph shows the difference spectrum. (For interpretation of the references to colour in this figure legend, the reader is referred to the web version of this article.)

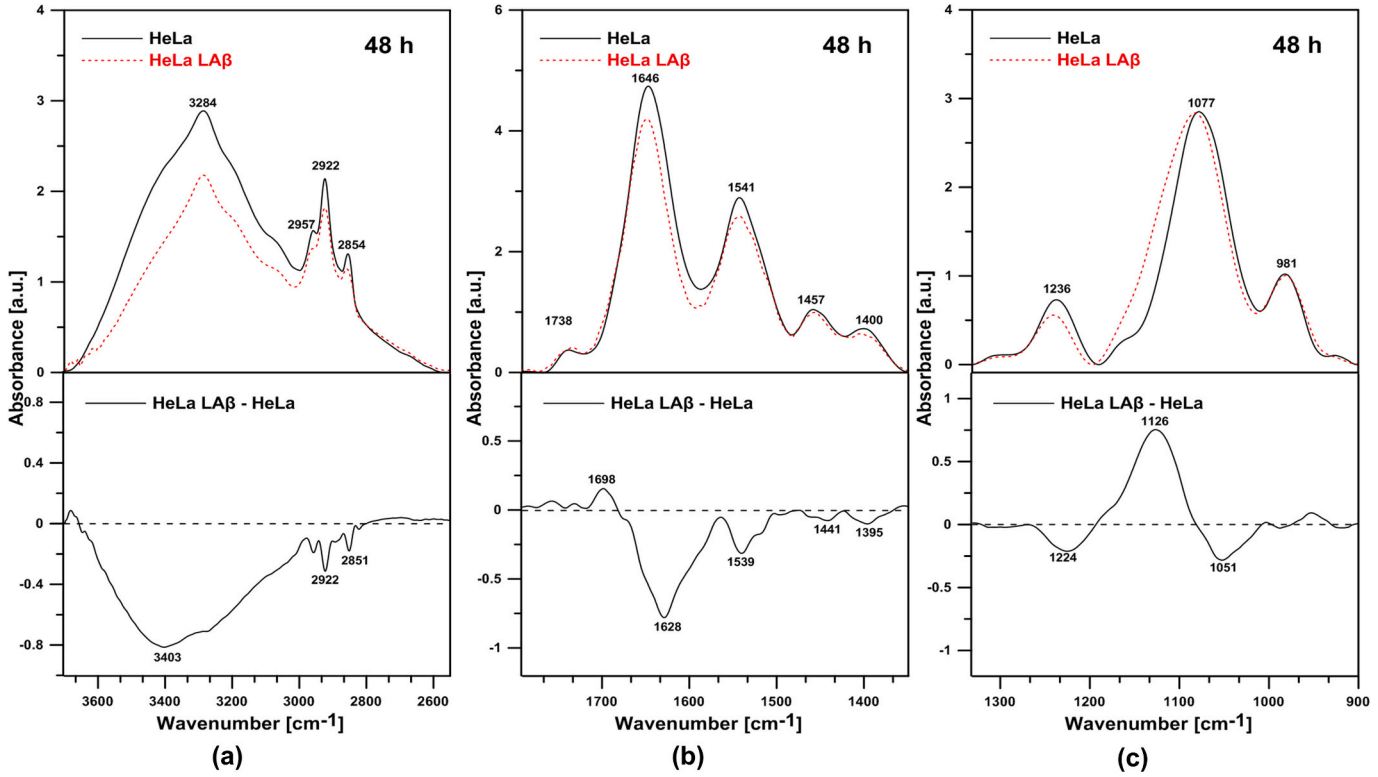

Fig. 5. FTIR spectra a) in the range 3800–2500 cm^{-1}, b) 2000-1300 cm^{-1} and 1300–900 cm^{-1} of untreated and treated with LAβ HeLa cells for 48 h. Difference spectra were presented at the bottom of the graph.

a decline in the absorbance of the peaks attributed to the symmetric and antisymmetric stretching vibrations of the CH_2 and CH_3 groups of the alkyl chains. In the band corresponding to an ester C = O stretching of phospholipids, a shift from 1738 cm^{-1} in control cells to 1733 cm^{-1} in cells treated with lensoside Aβ was revealed. Moreover, a decrease in intensity (a negative band in the difference spectrum with maximum at 1061 cm^{-1}) of the band characteristic of the symmetric stretching vibrations of the group - PO_{2-} was noted (Fig. 5c). Simultaneously a positive band at 1126 cm^{-1} in the difference spectrum was revealed (Fig. 5c).

Significant changes were noted in the area of amide I (1600–1700 cm^{-1}) and amide II (1510–1580 cm^{-1}) regions (Fig. 6). The intensity of the amide I and amide II bands decreased following a 48 h exposure. This indicates a reduction in relative protein concentration after incubation with lensoside Aβ. There was a decrease in the β-sheet (1627 cm^{-1}) with a simultaneous increase in the antiparallel β-sheet (1698 cm^{-1}, 1686 cm^{-1}) and turns (1667 cm^{-1}). The obtained results show that after a longer incubation time, the flavonoid inhibits protein synthesis and causes their partial denaturation.

3.3. *The effect of LAβ on viability of human cervix carcinoma cells*

The cytotoxic effect of LAβ on HeLa cells was determined by the NR and LIVE/DEAD assays. The NR method indicated that the examined compound exhibited slight cytotoxic activity. Dose-dependent inhibition of HeLa cell viability was observed. After 24 and 48 h of exposure to the flavonoid at a dose 15 μg/mL cell viability equalled 95 % and 96 % respectively, whereas at concentration 50 μg/mL was decreased to 89 % and 86 % (Fig. 7).

The LIVE / DEAD test is based on the different permeability of the membranes of viable and dead cells. Viable cells with undamaged cell membranes emit green fluorescence, while cells with damaged membranes (dead) are stained red. After lensoside Aβ treatment, a rise in the number of red stained cells was revealed (Fig. 8b and c). Shrunken cells with membrane blebbing (yellow arrows) were also observed (Fig. 8b and c). A dose-dependent decrease in the number of viable cells caused by Laβ was illustrated in Fig. 8d. After 24 h and 48 h incubation with the examined compound at the dose of 50 μg/mL, viability value was 81 % and 77 %, respectively (Fig. 8d).

3.4. *The effect of LAβ on the initiation of apoptosis and necrosis in HeLa cells*

The assessment of cell death in HeLa cells following incubation with LAβ was conducted by staining with fluorochromes: propidium iodide and Hoechst 33342 [40].

Cells showing the specific type of death were counted and presented relative to live cells. As shown in Fig. 9, treatment with the flavonoid resulted in a dose-dependent increase in apoptosis. LAβ at a concentration of 25 μg/mL induced 17 % of apoptosis and 3,7 % of necrosis. Following a 48-h incubation, the number of apoptotic cells increased in a dose-dependent manner (Fig. 9b). The highest level of apoptotic cells (15 %) was noted at 50 μg/mL. Simultaneously, a slight increase in necrotic cells was observed (3,5 %). This was accompanied by a 23 % depletion in cell viability as determined by the LIVE/DEAD assay (Fig. 8d).

To substantiate the aforementioned outcomes, flow cytometry analyses were conducted and are presented in Figs. 10 and 11. For the purpose of the analyses, the cells underwent double staining with the annexin V-FTIC and propidium iodide dyes. Application of LAβ caused a higher level of apoptosis. The number of apoptotic cells (quadrant Q2 An + / PI + − late apoptosis and quadrant Q4 An + / PI - early apoptosis) increased in a concentration-dependent manner. Compared to the control cells, the apoptosis rate increased from 0.72 % to 3.95 %, 5.46 %, 6.91 %, 8.26 % and 7.23 % after 24-h' incubation with 5, 10, 15, 25 and 50 μg/mL of LAβ, respectively (Fig. 10 b). The highest level of apoptosis was recorded at a dose of 25 μg/mL. At the same time, examined the flavonol slightly induced cell necrosis (quadrant Q1 An-PI +) from 0.82

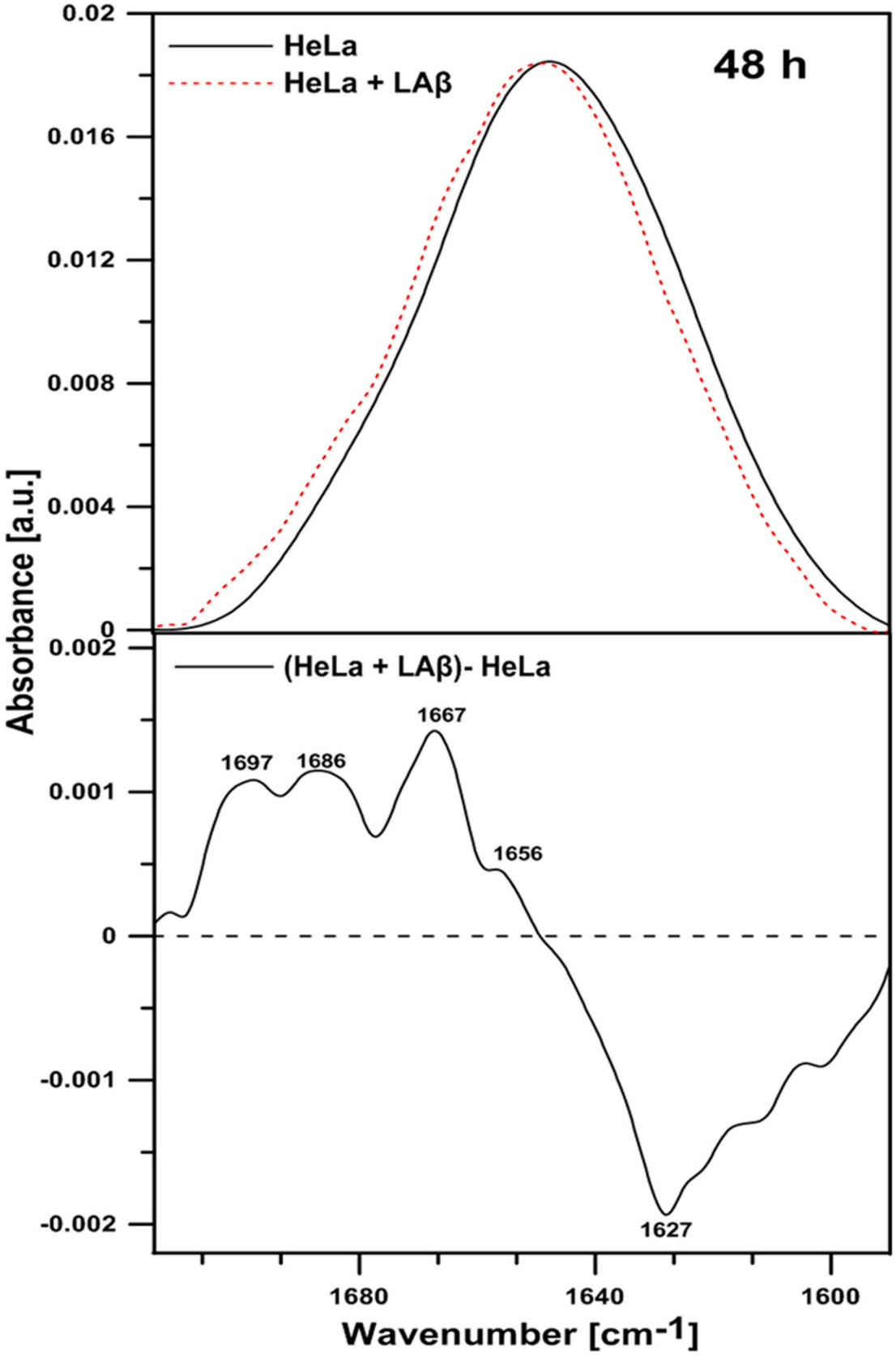

Fig. 6. Alterations in the protein's secondary structure after 48 h treatment with LAβ.

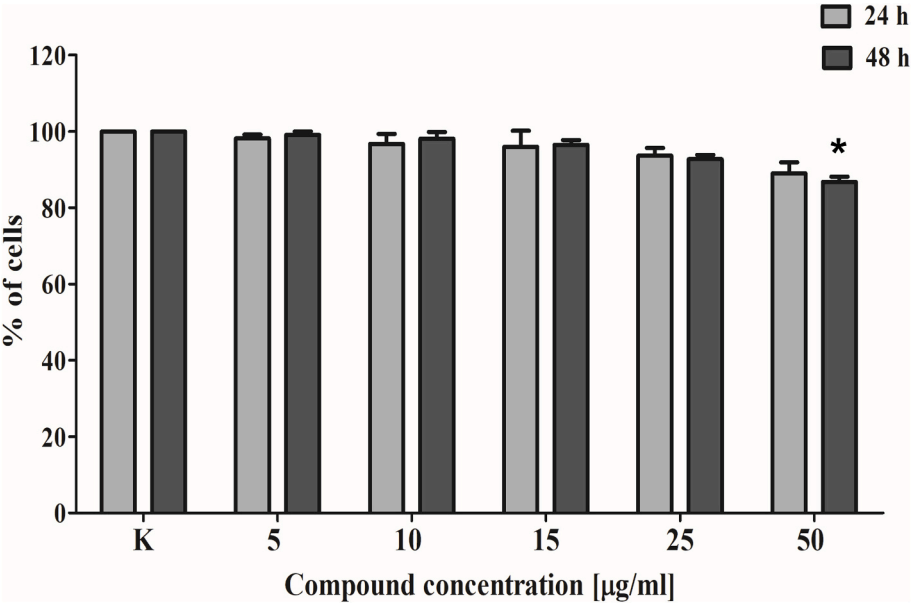

Fig. 7. Effect of lensoside Aβ on the viability of HeLa cells. The cell viability was assesed by the NR assay. The results represent the mean ± SD of tree independent experiments, *$p < 0.05$ in comparison to control, one- way ANOVA test.

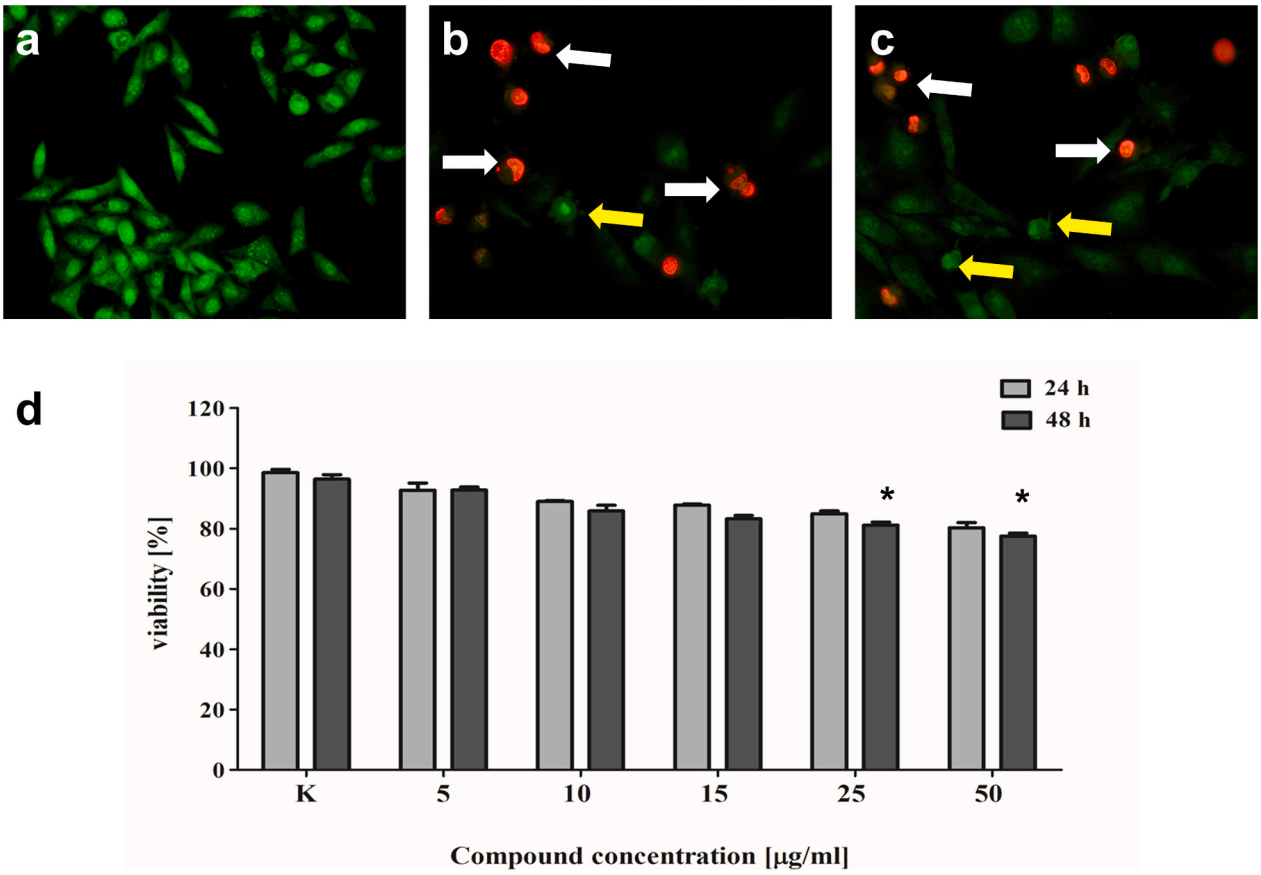

Fig. 8. Cytotoxic effect of lensoside Aβ on HeLa cells. a - control cells, b-c - HeLa cells treated with the tested flavonoid, damaged cell membranes are stained red (white arrows), shrink cells with numerous membrane vesicles (yellow arrows), d - percentage of alive cells after incubation with LAβ. Results are shown as means ± SD, $n = 3$; * $p \leq 0.05$; Student's *t*-test. (For interpretation of the references to colour in this figure legend, the reader is referred to the web version of this article.)

% in the control group to 2.38 % at a concentration of 50 µg/mL (Fig. 10b). Similar effects were obtained after 48 h of incubation with the tested flavonoid (Fig. 11). The most effective dose was the concentration of 25 µg/mL (9.18 ± 0.51 %). Additionally, a rise in the in quantity of necrotic cells n from 2 % to 4.4 % at the dose of 50 µg/mL was also noted.

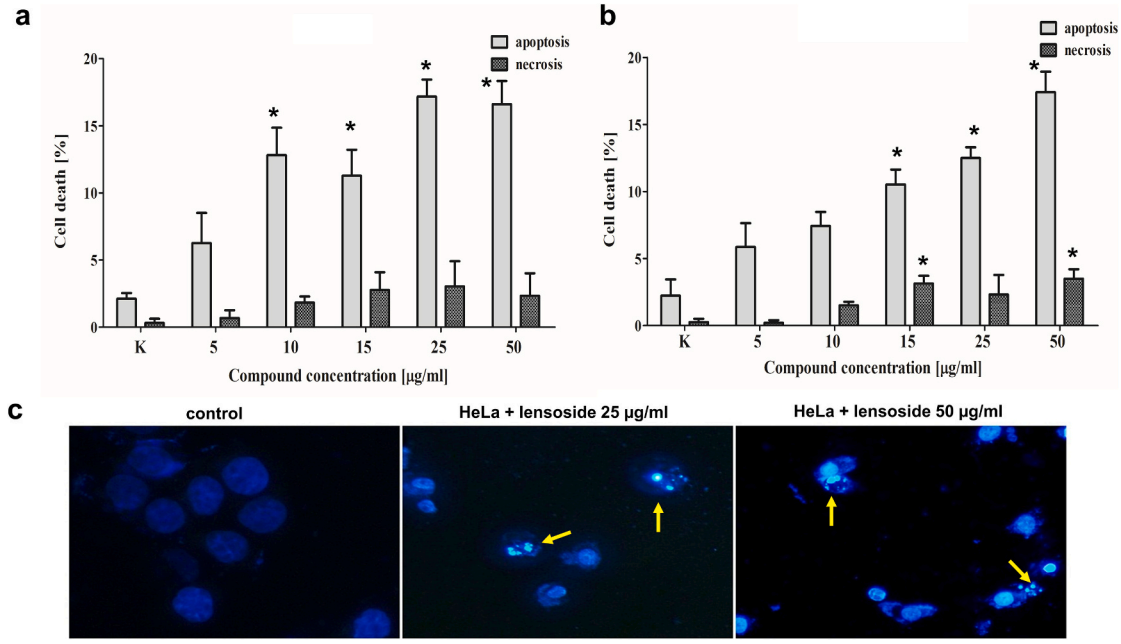

Fig. 9. The percentage of apoptotic and necrotic cells in HeLa cells treated with LAβ for 24 h (a) and 48 h (b). Results are presented as means ± SD, $n = 3$, * $p \leq 0.05$; Student's t-test. (c) Blue cells - normal (living) cells; cells showing intense blue fluorescence - apoptotic cells. Yellow arrows indicate apoptotic bodies. (For interpretation of the references to colour in this figure legend, the reader is referred to the web version of this article.)

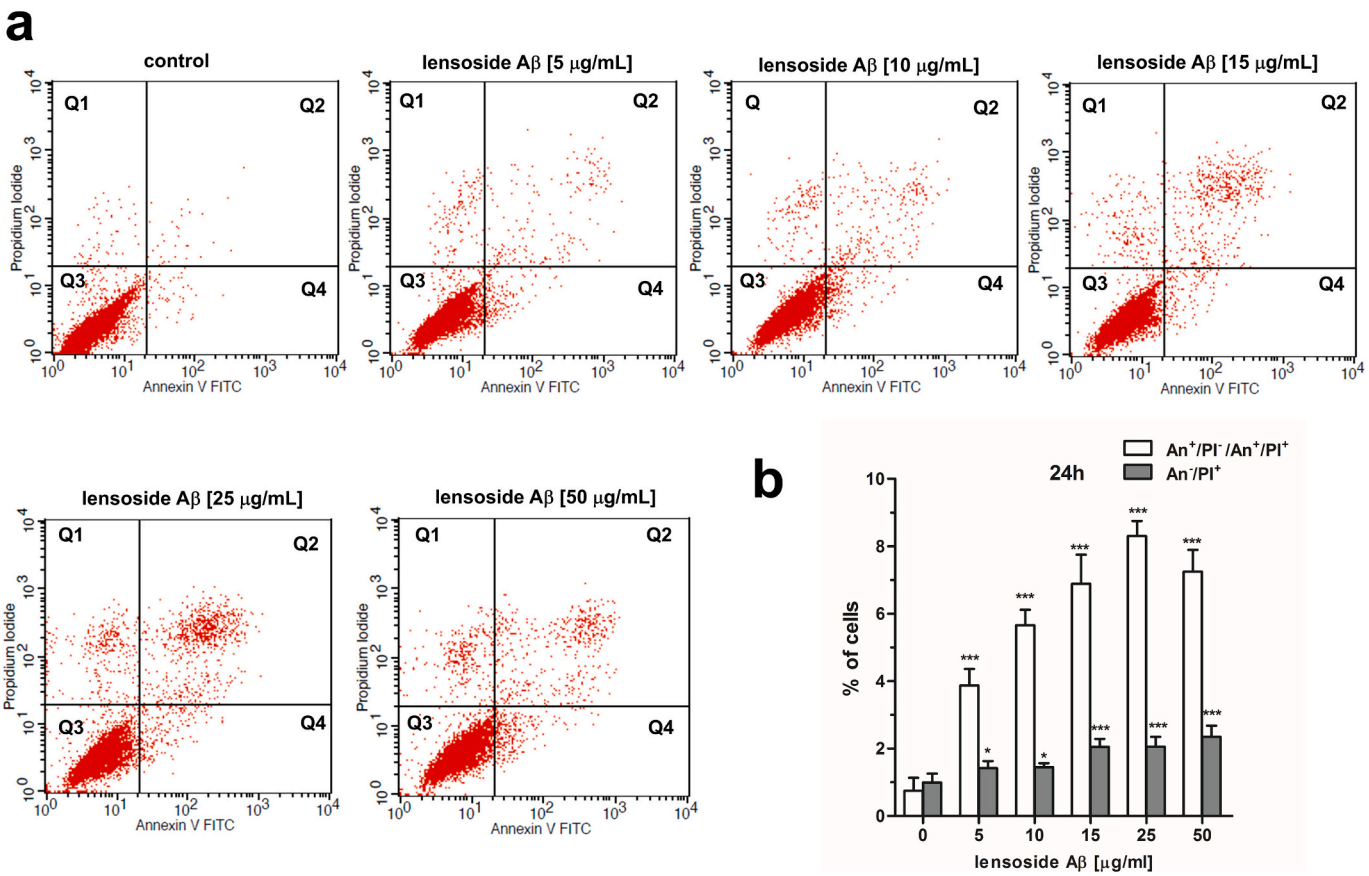

Fig. 10. a - Flow cytometry analysis of HeLa cells incubated with LAβ for 24 h at concentrations of 5, 10, 15, 25 and 50 μg/mL. Panel Q1 represents An-/PI+ cells dying via necrosis, Q2 - An+/PI+ cells dying by late apoptosis, Q3 - An-/PI- alive cells, Q4 - An+/PI- - cells in the early apoptosis stage. b– Perecentage of apoptotic and necrotic cells. Mean ± SD (n=3), statistically significant at $p \leq 0{,}1$; ** $p \leq 0{,}01$; *** $p \leq 0{,}001$ compared to the control cells; one-way ANOVA test.

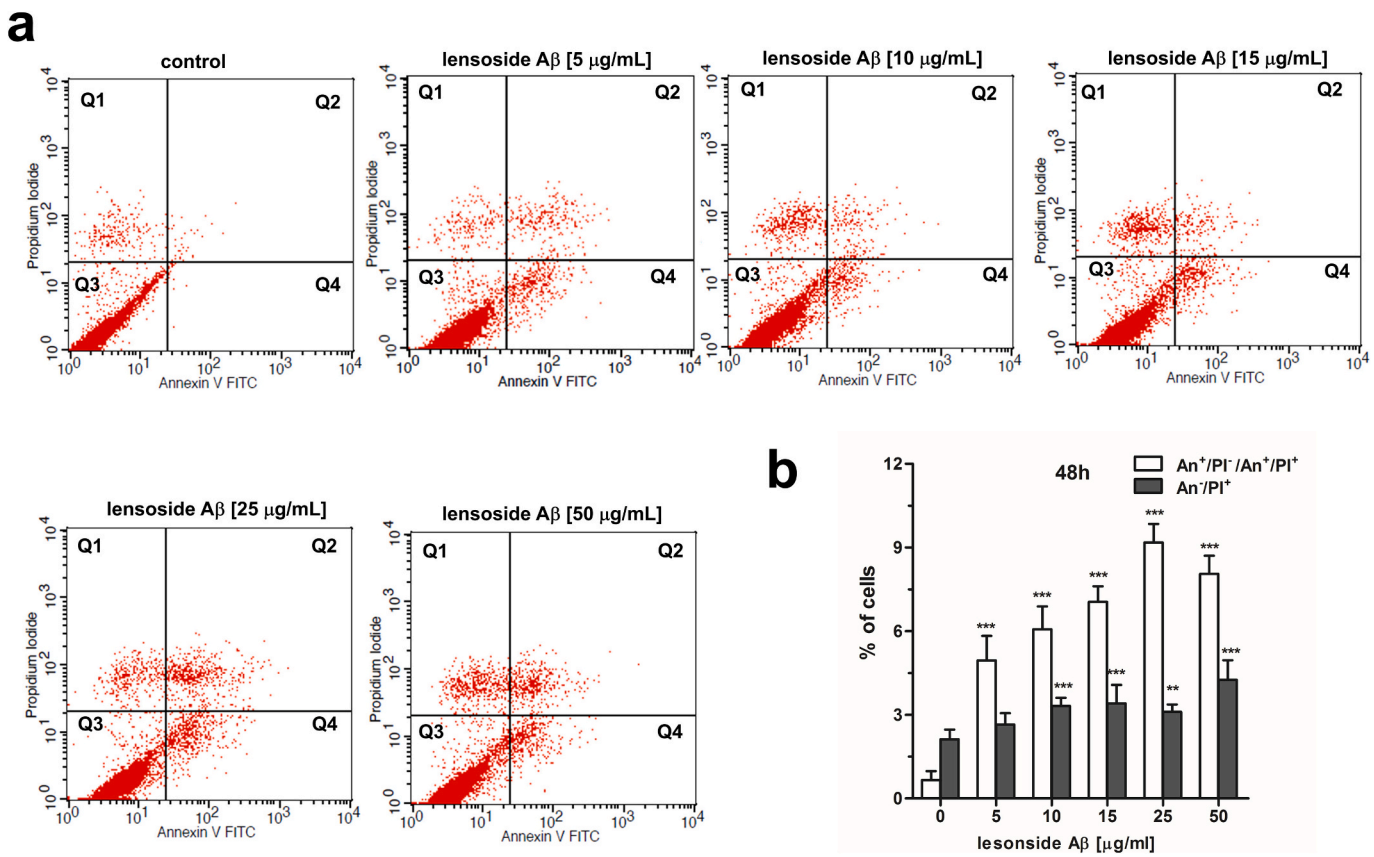

Fig. 11. a - Analysis of HeLa cells incubated with LAβ for 48 h at concentrations of 5, 10, 15, 25, 50 μg/mL by flow cytometry. Panel Q1 represents An-/PI+ cells dying via necrosis, Q2 - An+/PI+ cells dying by late apoptosis, Q3 - An-/PI- alive cells, Q4 - An+/PI- - cells in the early apoptosis stage. b– Perecentage of HeLa cells dying by apoptosis and necrosis. Mean ± SD (n=3); statistically significant at $p \leq 0,1$; ** $p \leq 0,01$; *** $p \leq 0,001$ compared to the control cells; one-way ANOVA test.

3.5. LAβ changes morphology, ultrastructure and morphometric parameters of human cervix carcinoma cells

To ascertain alterations in the morphology of HeLa cells treated with lensoside Aβ, a scanning electron microscope (SEM) was used. The cervical cancer cell culture was dense and adherent. The cells were elongated and flattened (Fig. 12a i 12b). They have exhibited the typical morphological characteristics, including a high density of microvilli on the cell surface and the presence of various structures, such as lamellipodia and filopodia (Fig. 12c). The cells were connected to one another via a series of processes.

After 24 and 48 h of incubation with the tested flavonoid, notable alterations in cell morphology and number were discerned. HeLa cells were sensitive to each of the compound concentrations that were used. Application of LAβ caused a decrease in the number of cells and a reduction of connections between them. The cells treated with the flavonoid were spherical and shrank (Fig. 12d, e, f, g). Significant changes in cell morphology, such as membrane blebbing, loss of microvilli, and the emergence of structures that resembling apoptotic bodies, were revealed (Fig. 12 h).

Further in this study, transmission electron microscope (TEM) was employed to demonstrate the effect of LAβ on the ultrastructure of HeLa cells. Fig. 13 shows the ultrastructure of control cells and cells exposed to flavonoid at dose 15 μg/mL for 24 h. In the control cells organelles of a typical appearance were observed. They had a large, centrally located, regular-shape nucleus with visible nucleoli and evenly dispersed chromatin. The nuclei had discernible membranes. The endoplasmic reticulum (ER) with well-preserved cisternae and ribosomes adjacent to its surface were visible. The microvilli of the cell membrane and the connections between the cells were clearly visible (Fig. 13a, b). A 24-h incubation of HeLa cells with LAβ caused a decrease in cell viability to 80,9 ± 2,5 %. Simultaneously, significant changes in the ultrastructure of cells exposed to the examined flavonoid were observed.The nuclei were irregularly shaped and shrunken, and chromatin was condensed and fragmented (Fig. 13d, f). Many small vesicles and big vacuoles with some dense material inside appeared in the cytoplasm (Fig. 13c). Cells treated with LAβ exhibited swollen mitochondria, membrane blebbing and reduced microvili (Fig. 13e). In some cells, changes characteristic for autophagy were observed.

Fig. 14 presents the morphometric parameters of HeLa cells before and after treatment with LAβ. The cells were exposed to the test compound at a dose of 15 μg/mL for 24 and 48 h. The dimensions of the cells and nuclei (diameter, perimeter and surface area) were measured.

Microscopic analyses showed that, in the HeLa cells, the addition of LAβ increased the number of cells with darker nuclei and condensed, dark cytoplasm. Conversely, the number of „light cells and nuclei" decreased compared to the control group (Fig. 14a). The conducted tests revealed a decreased perimeter in the examined cells. The mean perimeter in control light cells was 70.49 μm. In cells incubated with LAβ, the perimeter decreased to 68.39 μm. A similar change was observed in dark cells. In the flavonoid-treated cells, the perimeter was reduced by 2.3 % compared to the control. Reduction of dark and light nuclei perimeters was noted. Similar changes were observed after 48 h of incubation with the examined compound. LAβ decreased the perimeter of light and dark cells by 21,9 % and 24,7 %, respectively (Fig. 14c).

Another measured parameter was the diameter of the cells and nuclei. Treatment with lensoside Aβ for 24 h decreased the diameter of dark HeLa cells. In control, the average diameter of dark cells was 17.38 μm, whereas the diameter of the cells incubated with flavonoid, was 16.76 μm. The mean diameter of the dark nuclei was 8 % less than that

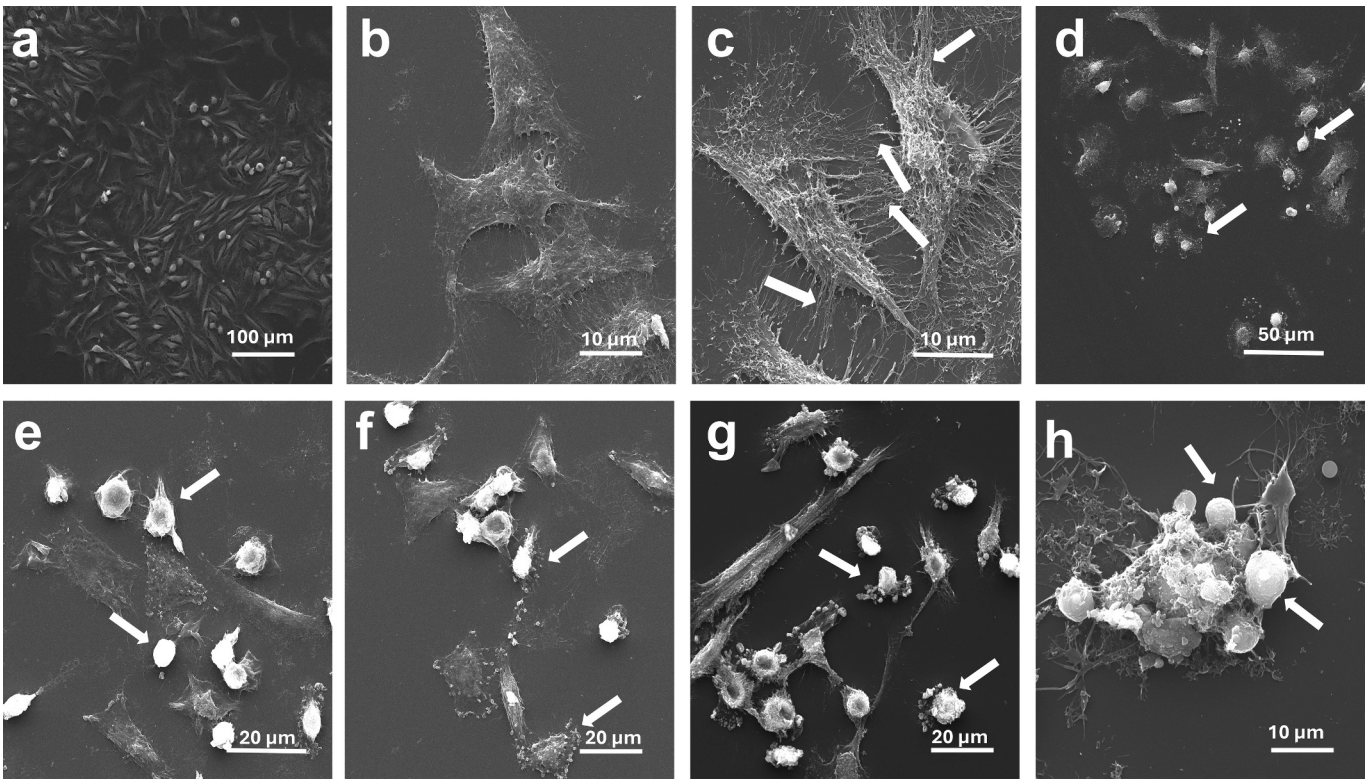

Fig. 12. HeLa cells investigated by scanning electron microscopy (SEM): a-c – control cells, d-h – cells incubated with LAβ; a – dense, flattened cells, b – adherent HeLa cells presenting microvilii on the surface, connections between neighbouring cells are visible, c – cells presenting microvili on the surface, processes connecting adjacent cells, d - shrunken HeLa cells (arrows), loss of connenctions between cells is visible, e - cells were shrunk and had a globular shape, loss of microvili was observed, f - after lensoside Aβ treatment loss of connections between adjacent cells and loss of microvili were revealed, g - HeLa cells showing blebs on the surface (arrows), h- HeLa cells exhibiting structures resembling apoptotic bodies (arrows).

observed in the control cells. No alteration was observed in this parameter with regard to light nuclei A similar trend was noted after long-time incubation. The diameters of dark cells and nuclei decreased by 28.3 % and 28.2 %, respectively (Fig. 14 b). Analysis showed a reduction in the average surface area of examined cells. In dark cells, surface areas were decreased by 56 %. The addition of LAβ also reduced the surface area of light cells and light and dark nuclei (Fig. 14d).

3.6. *LAβ induced oxidative stress in HeLa cells*

The study aimed to determine the effect of the tested compound on the induction of oxidative stress in in vitro cultured cells. Intense green mitochondrial fluorescence was observed in cells with high levels of reactive oxygen species (ROS). The results are presented as a percentage of cells showing increased free radical levels within the total population of the tested cells.

Lensoside Aβ induced oxidative stress, after both 24 and 48 h. After 24 h characteristic green mitochondrial fluorescence was observed in 32 % of the cells at the highest doses (25 and 50 µg/mL) (Fig. 15 a). Extending the incubation time increased the number of cells with high ROS levels, up to 40 % at 25 µg/mL (Fig. 15 b).

4. Discussion

The biological activity of compounds is related to their interaction with membranes. Therefore, in our study we attempted to estimate the effect of lensoside Aβ on a model membrane made with EYPC and on the lipid and protein components of HeLa cells. We then determined the effect of this compound on the morphology, ultrastructure, viability and apoptosis induction of HeLa cells.

4.1. *^{1}H NMR investigation*

The cell membrane is the first specific barrier for molecules entering the cell. Therefore, the interaction with the lipid bilayer and membrane proteins has a significant impact on the flavonoid's mechanism of action. The biological activity of compounds can be understood by considering two key factors: the way they interact with the membrane and their localization in the membrane [32]. Cell membranes are a primary target for anticancer and cancer chemopreventive agents [41]. To evaluate interaction of lensoside Aβ with liposomes made of EYPC the ^{1}H NMR technique was used. This technique is a useful tool for monitoring the dynamic and structural attributes of membranes. Due to the content of unsaturated acyl chains, EYPC membranes are less compact in their structure. Based on the literature, it is known that the membranes of normal cells are more rigid than those of cancer cells, especially invasive ones [42,43]. Accordingly, in this investigation we used liposomes formed with EYPC, to mimic the lipid phase of cancer cell membranes. The results obtained with this technique indicated that the examined compound had been integrated into the phospholipids' polar head group region. Moreover, a broadening of the band characteristic of the inner and outer layers of the polar head groups was observed, related to the restriction of the freedom of segmental movement in this area. In the presence of Laβ, a decrease in lipid movement freedom in the alkyl chain region of the EYPC liposomes was observed. These results are consistent with our previous findings regarding liposomes created with DPPC [29]. The incorporation of LAβ into DPPC liposomes also caused stiffening of the phospholipid polar zone and increased the value of the full width at half height of the peak attributed to -CH_2 groups in the hydrophobic region. Studies of EYPC liposomes using ^{1}H NMR and EPR techniques showed that another flavonoid - genistein also decreased the movement freedom in the hydrophilic region [44]. Our results obtained

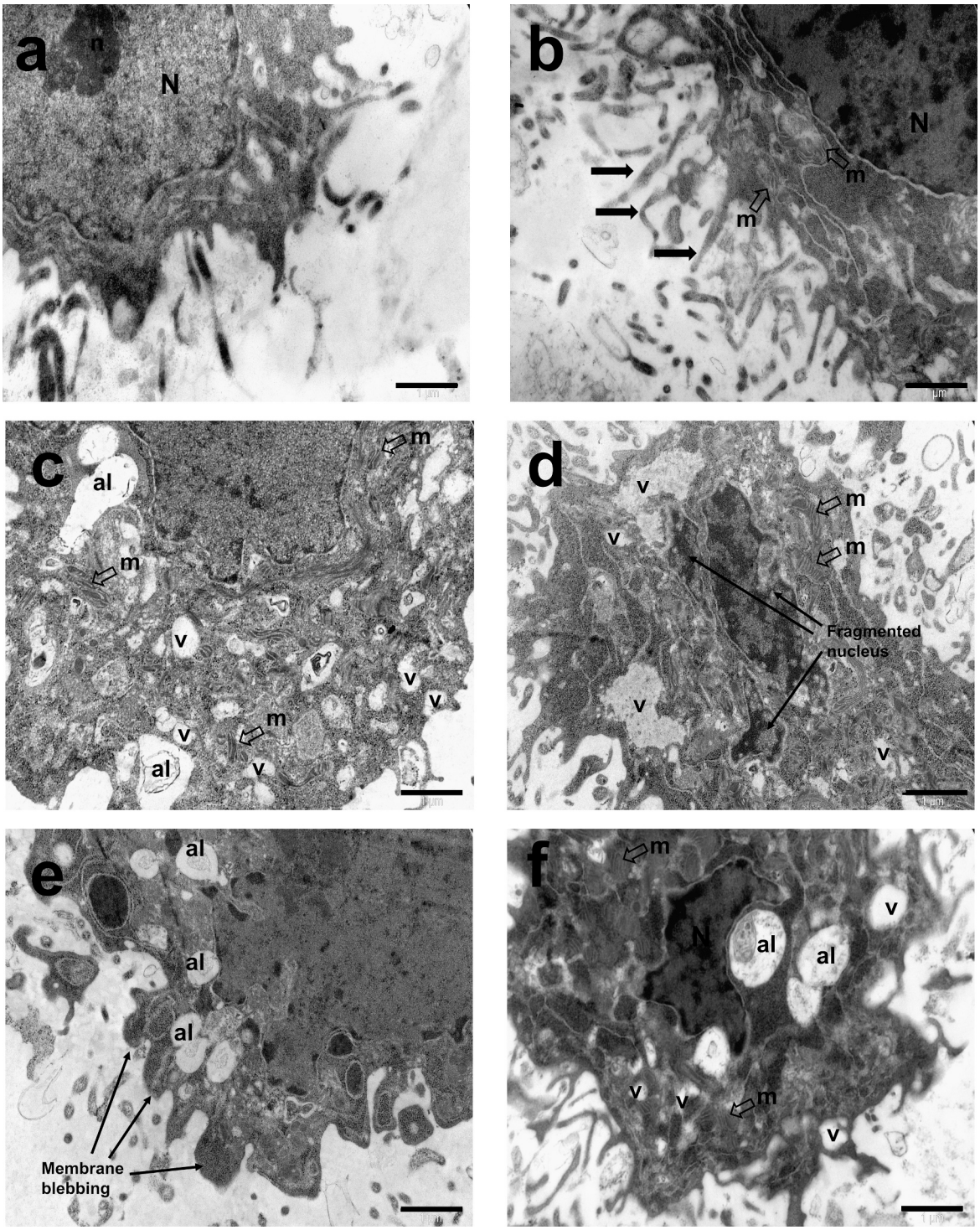

Fig. 13. Ultrastructure of HeLa cells examined by TEM: a-b – control cells, c-f – cells exposed to lensoside Aβ at concentration 15 μg/mL for 24 h. a- b– Untreated cells with mitochondria (m) and a large centrally located nucleus (N) with visible nucleolus (n). Black arrows indicate numerous microvilli. c – Fragment of HeLa cells with an irregularly shaped nucleus (N) visible, strong vacuolization (v), numerous condensed mitochondria (m) and autolisosomes (al), d – HeLa cells after treatment with LAβ with a irregularly shaped, and fragmented nucleus (N) and condensed chromatin. Large vacuoles (v) were noted. e – Cells exposed to the tested flavonoid with and autolisosomes (al). Membrane blebbing is visible (black arrows). f – HeLa cells presenting a shrunken nucleus (N), autolisosomes (al) and small vacuoles (v).

with the ^{1}H NMR technique are partially in agreement with studies on the effect of quercetin (of which lensoside Aβ is a derivative) on DPPC membrane. Quercetin is located in the polar-nonpolar interface and also caused rigidity with respect to the polar region of the membranes. On the other hand, quercetin increased the motional freedom of lipids in the alkyl chain region [45]. A distinct effect of the tested compound on the fluidity of the hydrophobic region may be due to the difference in the lipid composition of liposomes and the structure of the quercetin derivative (presence of sugar moieties and caffeic acid). Besides, the splitting parameter (δ) has increased from 0.19 to 0.20 ppm. This is due to the fact that LAβ was incorporated into the polar zone, increasing the penetration of Pr^{3+} ions into this region.

Our findings prove that the presence of lensoside Aβ has an ordering effect on liposomes made with EYPC, which may be important for its

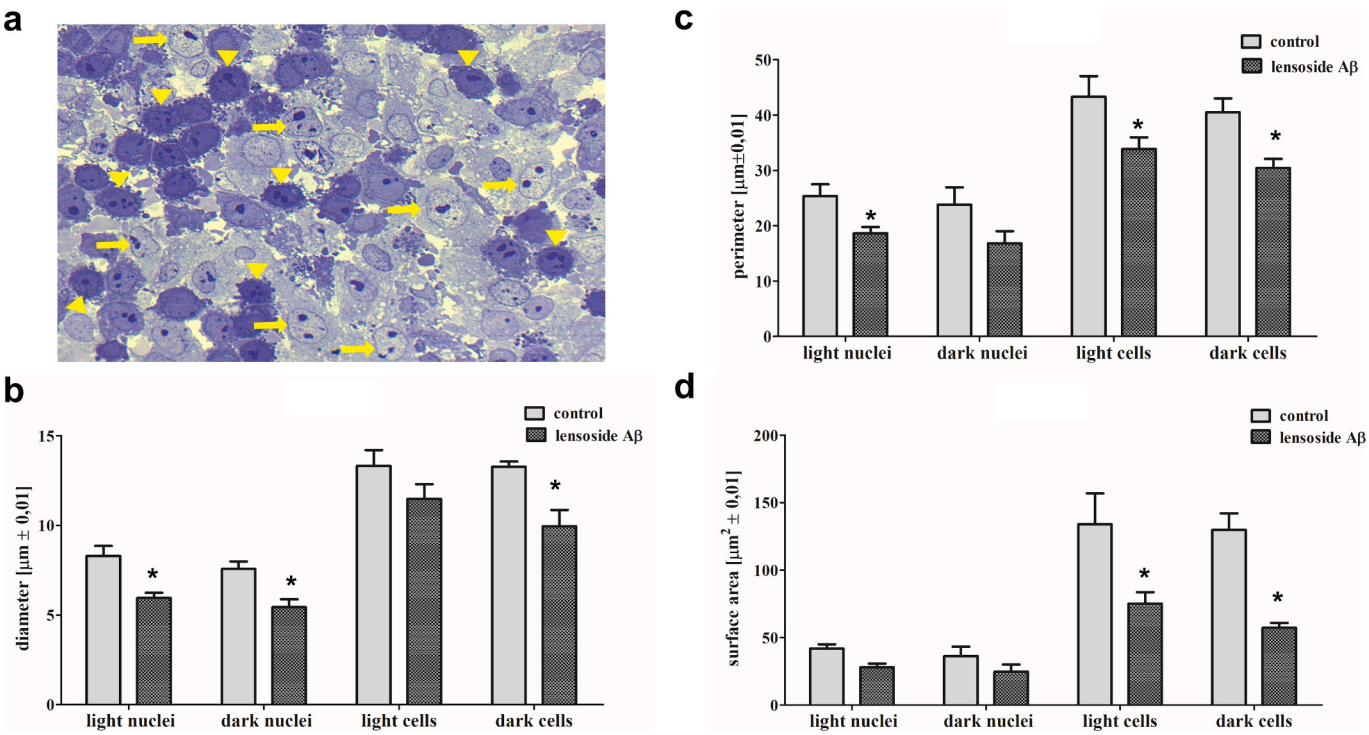

Fig. 14. Alterations in the dimensions of HeLa cells and nuclei after treatment with LAβ. a – A representative image of a semithin section of the tested cells exposed to the flavonoid, yellow arrows show light cells with nuclei, yellows arrowheads indicate dark shrunk cells. b – d - An analysis of HeLa cells and nuclei dimensions (diameter, perimeter and surface area). (For interpretation of the references to colour in this figure legend, the reader is referred to the web version of this article.)

anticancer properties. Based on the available literature, it is known that changes in membrane fluidity affect cell proliferation, the cell cycle and the initiation of apoptotic death. Neoplastic and metastatic cell membranes are more fluid than normal cell membranes, therefore membrane-rigidifying compounds would prevent the increased membrane fluidity of tumor cells. Consequently, altering the fluidity of membranes disrupts the conformation of enzymes and receptors that are important in tumorigenesis [33].

4.2. *Lensoside Aβ effect on cellular components of HeLa cells*

Subsequently, we employed the FTIR spectroscopy to investigate whether the tested flavonoid cause changes in the spectral profiles of the proteins and lipids in cervical cells. FTIR spectroscopy is a highly sensitive tool that enables the analysis of chemical modifications in cellular components (e.g., proteins, nucleic acids, and lipids) [46]. This technique has been used by many researchers to study the interactions of bioactive compounds with cells and tissues [47–52]. Incubation with lensoside Aβ resulted in strong decrease in the oscillator strength of the amide I and amide II bands, indicating a reduction in relative protein concentration. During apoptosis existing proteins are modified and the new proteins are synthesized [53,54]. This is why we decided to analyze in detail the amide I area. The examined compound altered the spectral profile of the proteins in the HeLa cells in this region. Cells treated with flavonoids for 24 h exhibited lower levels of turns and α-helices, accompanied by higher levels of β-sheets. In turn, after a longer incubation time an increase in antiparallel β-sheets and turns and a decrease in β-sheets were noted. Such results may indicate the fact that after a longer incubation time, this compound inhibits protein synthesis and causes their partial denaturation. Cleavage of proteins by caspases changes in proteasome function and chaperone activity could change protein levels and affect their folding and localization. This, in turn influences the IR absorption of peptide bonds [55].

Similar results were obtained by researchers investigating the effects of the natural product with anticancer activity (PM 701) on human lung cancer cells (A549). In the initial stages of apoptosis, the amount of β-sheets increases, while after a longer incubation time an increase in disordered structures was observed [56]. In turn, Elmadany and colleagues' studies on the synergy of doxorubicin and quercetin on the MCF-7 breast cancer cell line showed that the combined therapy with these two compounds reduced the protein concentration and changed the amide I region. At the same time, there was an increase in the number of β-sheet aggregates, and a decrease in the number of α-helix structures. A combination of quercetin and doxorubicin caused abnormal folding of proteins in MCF-7 cells and their aggregation, which in consequence induced apoptosis [57].

The phospholipids in the plasma membrane determine the membrane fluidity, stability and enzymatic activity [58]. Therefore, monitoring changes in lipid absorbance is relevant for detecting apoptosis. Following LAβ treatment a positive peak in the difference spectrum with a maximum at 1747 cm^{-1} corresponding to ester C═O stretching vibrations of phospholipids was observed. Furthermore, the band contributing to the asymmetric stretching vibrations of the acyl chain CH_3 groups with a maximum at 2957 cm^{-1} and the bands at 2854 cm^{-1} and 2922 cm^{-1} assigned to the symmetric and asymmetric stretching vibrations of the acyl chain CH_2 groups were negative. This can be interpreted as a decline in HeLa cells membrane lipid levels and/or structural changes of phospholipids after LAβ treatment [53,59]. Many authors suggest that membrane changes such as phosphatidylserine exposure and membrane blebbing are linked to an increase in lipids in cells undergoing apoptosis [60]. However, in some investigations, a decrease in intensity of lipid bands in apoptotic cells was observed [55].

The present investigation has also revealed significant changes in the 1300 and 900 cm^{-1} regions assigned to phosphates in phospholipids and DNA. After, treatment with LAβ for 24 h the bands corresponding to the symmetric stretching of phosphodiester groups at 1082 cm^{-1} were strengthened. Such an effect can be explained by the incorporation and interaction of the tested flavonol with the polar zone of the phospholipids. These conclusions are confirmed by the ^1H NMR results and our previous study on DPPC liposomes [29]. The area sensitive to hydrogen

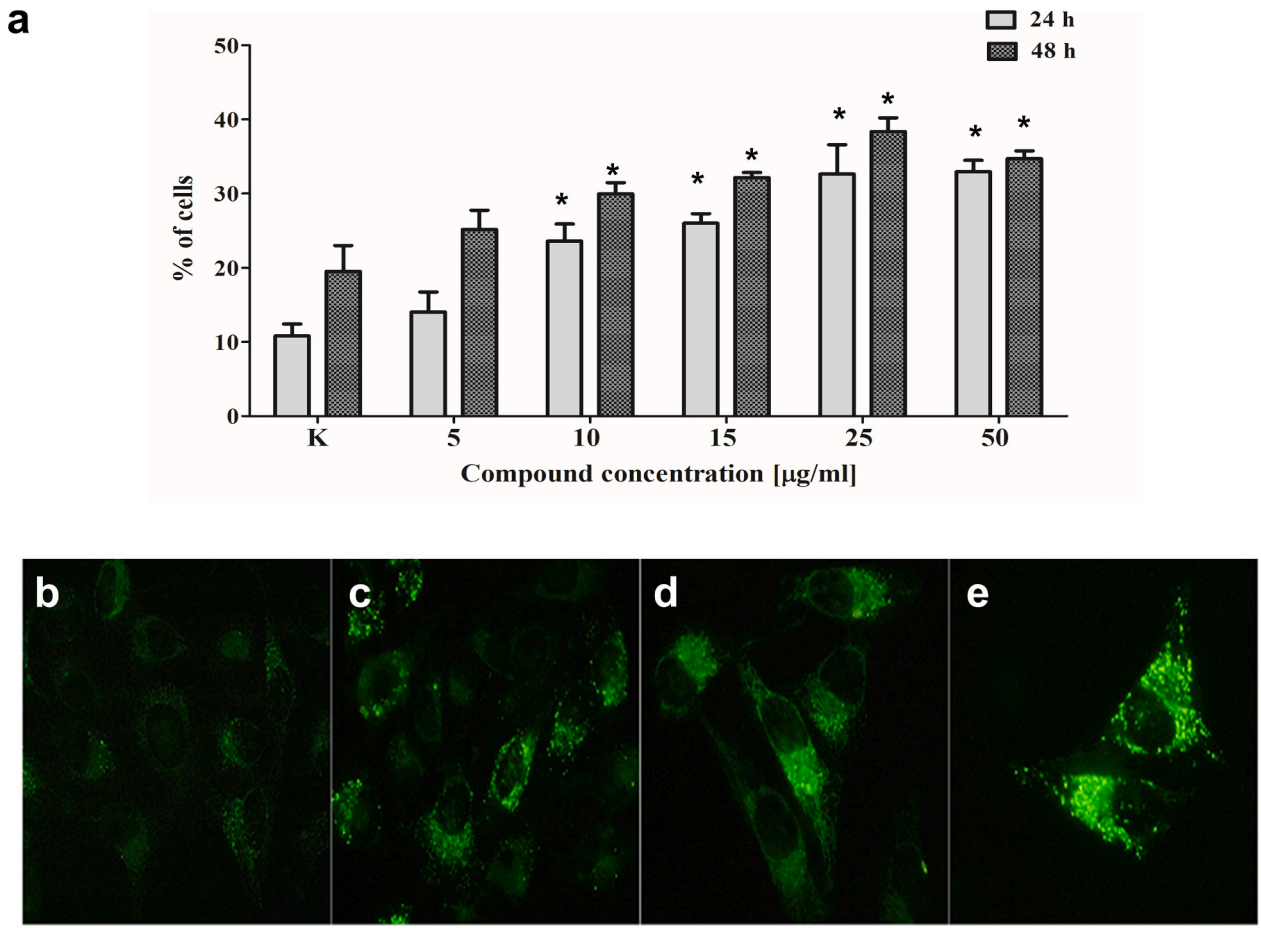

Fig. 15. Induction of oxidative stress in HeLa cells following exposure to LAβ for 24 and 48 h. a- the bars represents the average level of reactive oxygen species (ROS) after treatment with the flavonoid; b – control HeLa cells, c-e – HeLa cells after treatment with Laβ. Intensive green fluorescence was observed in cells with high levels of ROS. (For interpretation of the references to colour in this figure legend, the reader is referred to the web version of this article.)

bonding and interactions with compounds is the region of the symmetric vibrations of the stretching groups - PO_{2-} [39]. In addition, numerous studies have shown that flavonoids binding via hydrogen bonds to polar head groups of phospholipids [29,35,61,62]. The region with a maximum of 1082 cm^{-1} is also known to be related to cell nucleic acids [55,63]. As a result the action of drugs in the cells, there are changes to the DNA that are visible as alteration in the absorption intensity of bands in the 1300–900 cm^{-1} region [55]. Our research showed that, after 48 h LAβ caused a slight decrease in the oscillator strength of the band characteristic of the symmetric stretching of - PO_{2-} groups, which are found also in DNA. This decrease was observed as a negative band at 1061 cm^{-1} in the difference spectrum. Many authors have suggested that low intensity in the nucleic acid's region is related to apoptosis [55,64–66]. During apoptosis DNA is compacted and absorbs less IR [60].

4.3. LAβ alters the morphology, ultrastructure and viability of human cervix carcinoma cells

In our investigation we determined the cytotoxic activity of LAβ against human cervical carcinoma cells. The results obtained with the neutral red (NR) test and the LIVE / DEAD tests were consistent and showed a decrease in cell viability. Simultaneously, fluorescent microscopy and flow cytometry analyses revealed that the application of the tested compound led to apoptosis in approximately 15 % of cells. Additionally, changes in morphology and ultrastructure characteristic of apoptosis under SEM and TEM microscopes were observed. Control cells have exhibited the expected morphological characteristics, including the presence of dense microvilli and many structures such as lamellipodia and filopodia. The presence of filopodia and microvilli indicates the invasive potential of cancer cells and is a key factor in their migratory capacity. Application of LAβ caused significant changes in cells morphology, such as membrane blebbing, loss of microvilli, formation of apoptotic vesicles, and reduction of connections between cells. The cells treated with the flavonoid were spherical and shrunk. The tested flavonoid is a quercetin glycoside [17]. Numerous literature data show that quercetin exhibits highly cytotoxic activity and induces apoptosis of different types of cancer, including gastric cancer [67], breast cancer [68], colorectal cancer [69], oral cavity cancer [70], liver cancer [71], prostate cancer [72], thyroid cancer [73], leukaemia [74], pancreatic cancer [75] and lung cancer [76]. At the same time, an increasing number of investigations indicate that quercetin promotes the apoptotic death of cervical cancer cells [77–79].

The data obtained by Zhang and co-researchers corresponds with our findings. They revealed changes in the morphology of cervical cancer cells and initiation of their apoptosis after quercetin treatment. Cell shrinkage, a reduction in the number of microvilli and the formation of apoptotic bodies were observed [80]. Changes characteristic for apoptosis cells were also found by Talib and colleagues who studied the effects of methyl quercetin derivatives isolated from *Inula viscosa* on MCF-7 cells. Similarly to our study, the cells exposed to flavonoids were shrunken and had fewer microvilli. Membrane blebbing, and the loss of contact between adjacent cells as well as the formation of apoptotic bodies were observed [81]. In addition, other researchers found that flavonoids caused cell shrinkage and a reduction or complete loss of microvilli [82]. Alterations of cell morphology can be explained by their

effect on cytoskeleton proteins. In our experiments, we proved that LAβ decreased the protein level in HeLa cells and changed their spectral profile. Additionally, modifications to cells morphology were identified. TEM observations showed that examined flavonoid induced alterations in the ultrastructure of the tested cells. This results are consistent with our outcomes obtained with SEM. The nuclei were irregularly shaped and shrunken, and chromatin was condensed and fragmented. Swollen mitochondria appeared in the cytoplasm. The cells exhibited intense vacuolization. Morphometric measurements revealed a decrease in the perimeter, diameter and surface area of the cells. In the presence of flavonoid an increased number of dark cells characterized by dense cytoplasm and condensed chromatin were observed. The results of Priyadarsini and co-author's support our data. They found that HeLa cells exposed to quercetin were shrunken, exhibited condensed chromatin and fragmented nuclei [83]. The findings of other researchers were also in accordance with our observations. They demonstrated that quercetin promotes apoptosis and inhibits the cell cycle in the G2/M phase, resulting in chromatin condensation and DNA fragmentation [84]. Cells treated with quercetin exhibited numerous vacuoles, condensed chromatin and membrane blebbing [85].

4.4. Prooxidative activity of LAβ

The latest research has shown that the anti-cancer effects of some flavonoids may be related to their pro-oxidative properties. Flavonoids, by increasing the level of ROS, activate apoptotic, necrotic and autophagic pathways and reduce tumor size [86].These compounds may induce apoptosis in cancer cells by disrupting the oxidative processes in cells, generating reactive oxygen species (ROS) or modulating detoxifying enzymes [87–89]. Due to the fact that one of the mechanisms of flavonoids action is related to their pro-oxidative properties, the influence of LAβ on the level of ROS was investigated. Our study showed that the flavonoid induces apoptosis in HeLa cells. Moreover, the examined compound increased the level of ROS by 20 % compared to the control cells. Our observations are supported by the findings of other researchers. Similarly, quercetin may alter ROS metabolism and induce apoptosis. Bishayee and coauthors found that quercetin inhibits the cell cycle and induces apoptosis in HeLa cells by ROS accumulation and release of cytochrome *c* [90]. In Hep2G2 and HA22T/VGH cells, a high concentration of flavonol, generates free radicals after a longer incubation time. As a consequence, disruption of the mitochondrial membrane potential, release of cytochrome *c*, and apoptosis induction were revealed [91]. Furthermore, quercetin causes ROS-mediated apoptosis in prostate [92,93], gastric [94] and colon cancer cell lines [95]. It can also be used in combination therapy with other chemotherapeutic agents. Quercetin by accumulating ROS, enhances the anticancer activity of paclitaxel on prostate cancer cells [96].

5. Conclusions

The therapeutic effect of drugs, such as plant compounds, is directly linked to their incorporation into the lipid bilayer and the modification of membrane fluidity, as well as their impact on cell proteins. In order to comprehend the molecular mechanisms of action of flavonoids, which are crucial in the treatment of many diseases, it is imperative to explain their interactions with membranes and their effect on membrane proteins. Changes in membrane fluidity may affect the cell cycle and apoptosis in cancer cells. For this reasons we have undertaken comprehensive studies. Cancer cells membranes exhibit greater fluidity than normal cells. Therefore, we investigated the effect of lensoside Aβ on liposomes made of egg yolk phosphatidylcholine (EYPC), which mimics the lipid phase of cancer membranes. We revealed that the examine compound incorporates into the polar head region of unsaturated membranes and restricts motility in this zone. In HeLa cells, the regions between 900 and 1300 cm^{-1} and amide I were targets for flavonoid. LAβ decreased the relative protein concentration and modified the secondary structure of proteins. Notable decrease in β-sheets accompanied by an increase in antiparallel β-sheets and turns were observed in the amide I area. Lensoside Aβ reduced the viability of HeLa cells and caused apoptosis. Moreover, changes in cell morphology and ultrastructure consistent with apoptosis were evident. Our studies have also confirmed the prooxidant activity of LAβ. The level of ROS after treatment with examined compound increased by 20 % compared to the control cells. The obtained outcomes indicate that lensoside Aβ by affecting the protein and lipid components of HeLa cells, could be a promising therapeutic agent.

CRediT authorship contribution statement

Justyna Kapral-Piotrowska: Writing – review & editing, Writing – original draft, Visualization, Validation, Supervision, Resources, Methodology, Investigation, Conceptualization. **Agata Wawrzyniak:** Supervision, Methodology, Investigation. **Jarosław Pawelec:** Supervision, Resources, Methodology, Investigation. **Barbara Zarzyka:** Supervision, Resources, Methodology, Investigation. **Roman Paduch:** Supervision, Methodology, Investigation. **Jerzy Żuchowski:** Supervision, Methodology. **Adrianna Sławińska-Brych:** Supervision, Methodology, Investigation. **Barbara Zdzisińska:** Supervision, Methodology, Investigation. **Bartłomiej Pawlęga:** Visualization, Supervision. **Alicja Wójcik-Załuska:** Visualization, Supervision. **Ewa Baranowska-Wójcik:** Validation, Supervision, Methodology. **Joanna Jakubowicz-Gil:** Validation, Supervision, Resources. **Wiesław I. Gruszecki:** Visualization, Supervision, Methodology, Investigation. **Bożena Pawlikowska-Pawlęga:** Writing – review & editing, Writing – original draft, Visualization, Validation, Supervision, Resources, Project administration, Methodology, Investigation, Funding acquisition, Data curation, Conceptualization.

Declaration of competing interest

The authors declare that they have no known competing financial interests or personal relationships that could have appeared to influence the work reported in this paper.

References

[1] K. Sak K, Characteristic features of cytotoxic activity of flavonoids on human cervical Cancer cells, Asian Pac. J. Cancer Prev. 15 (2014) 8007–8018, https://doi.org/10.7314/apjcp.2014.15.19.8007.
[2] C. Marth, F. Landoni, S. Mahner, M. McCormack, A. Gonzalez-Martin, N. Colombo, ESMO guidelines committee, cervical cancer: ESMO clinical practice guidelines for diagnosis, treatment and follow-up, Ann. Oncol. 1 (28) (2017) iv72–iv83, https://doi.org/10.1093/annonc/mdx220.
[3] M. Dürst, L. Gissmann, H. Ikenberg, H. Zur Hausen, A papillomavirus DNA from a cervical carcinoma and its prevalence in cancer biopsy samples from different geographic regions, Proc. Natl. Acad. Sci. USA 80 (1983) 3812–3815, https://doi.org/10.1073/pnas.80.12.3812.
[4] D. Sawaryn D, A. Wróbel, Young girls' knowledge's level concerning cervical cancer, Medycyna Rodzinna 2 (2011) 35–42.
[5] D.O. Garcia, C.A. Thomson, Physical activity and Cancer survivorship, Nutr. Clin. Pract. 29 (6) (2014) 768–779, https://doi.org/10.1177/0884533614551969.
[6] M.J.R. Howes, M.S.J. Simmonds, The role of phytochemicals as micronutrients in health and disease, Curr. Opin. Clin. Nutr. Metab. Care 17 (6) (2014) 558–566, https://doi.org/10.1097/MCO.0000000000000115.
[7] C. Rice-Evans, Flavonoid antioxidants, Curr. Med. Chem. 8 (7) (2001) 797–807, https://doi.org/10.2174/0929867013373011.
[8] E.L. Santos, B.H.L.N.S. Maia, A.P. Ferriani, S.D. Teixeira, Flavonoids: classification, biosynthesis and chemical ecology, flavonoids-from biosynthesis to human, Health 13 (2017) 78–94, https://doi.org/10.5772/67861.
[9] M.K. Sundaram, R. Raina, N. Afroze, K. Bajbouj, M. Hamad, S. Haque, A. Hussain, Quercetin modulates signaling pathways and induces apoptosis in cervical cancer cells, Biosci. Rep. 39 (2009) 1–17, https://doi.org/10.1042/BSR20190720.
[10] R.J. Nijveldt, E. van Nood, D.E. van Hoorn, P.G. Boelens, K. van Norren, P.A.M. van Leeuwen, Flavonoids: a review of probable mechanisms of action and potential applications, Am. J. Clin. Nutr. 74 (2001) 418–425, https://doi.org/10.1093/ajcn/74.4.418.
[11] M. Ferrali, C. Signorini, B. Caciotti, L. Sugherini, L. Ciccoli, D. Giachetti, M. Comporti, Protection against oxidative damage of erythrocyte membranes by the flavonoid quercetin and its relation to iron chelating activity, FEBS Lett. 416 (2) (1997) 123–129, https://doi.org/10.1016/s0014-5793(97)01182-4.

[12] C. Sandoval-Acuña, J. Ferreira, H. Speisky, Polyphenols and mitochondria: an update on their increasingly emerging ROS-scavenging independent actions, Arch. Biochem. Biophys. 559 (1) (2014) 75–90, https://doi.org/10.1016/j.abb.2014.05.017.

[13] L. Gibellini, M. Pinti, M. Nasi, S. De Biasi, E. Roat, L. Bertoncelli, A. Cossarizza, Interfering with ROS metabolism in Cancer cells: the potential role of quercetin, Cancers 2 (2010) 1288–1311, https://doi.org/10.3390/cancers2021288.

[14] G.C. Yen, P.D. Duh, H.L. Tsai, S.L. Huang, Pro-oxidative properties of flavonoids in human lymphocytes, Biosci. Biotechnol. Biochem. 67 (2003) 1215–1222, https://doi.org/10.1271/bbb.67.1215.

[15] M. Matsuo, N. Sasaki, K. Saga, T. Kaneko, Cytotoxicity of flavonoids toward cultured normal human cells, Biol. Pharm. Bull. 28 (2) (2005) 253–259, https://doi.org/10.1248/bpb.28.253.

[16] K. Ganesan, B. Xu, Polyphenol-rich lentils and their health promoting effects, Int. J. Mol. Sci. 18 (11) (2017) 2390, https://doi.org/10.3390/ijms18112390.

[17] J. Żuchowski, Ł. Pecio, A. Stochmal, Novel flavonol glycosides from the aerial parts of lentil (*Lens culinaris*), Molecules 19 (2014) 18152–18178, https://doi.org/10.3390/molecules191118152.

[18] G.E.A. Costa, K.S. Queiroz-Monici, S.M.P.M. Reis, A.C. de Oliveira, Chemical composition, dietary fibre and resistant starch contents of raw and cooked pea, common bean, chickpea and lentil legumes, Food Chem. 94 (2006) 327–330, https://doi.org/10.1016/j.foodchem.2004.11.020.

[19] M. Margier, S. Georgé, N. Hafnaoui, D. Remond, M. Nowicki, L. Du Chaffaut, M. J. Amiot, E. Reboul, Nutritional composition and bioactive content of legumes: characterization of pulses frequently consumed in France and effect of the cooking method, Nutrients 10 (11) (2018) 1668, https://doi.org/10.3390/nu10111668.

[20] R. Amarowicz, I. Estrella, T. Hernández, M. Dueñas, A. Troszyńska, A. Kosińska, R. B. Pegg, Antioxidant activity of a red lentil extract and its fractions, Int. J. Mol. Sci. 10 (2009) 5513–5527, https://doi.org/10.3390/ijms10125513.

[21] R. Amarowicz, I. Estrella, T. Hernández, S. Robredo, A. Troszyńska, A. Kosińska, R. B. Pegg, Free radical-scavenging capacity, antioxidant activity, and phenolic composition of green lentil (Lens culinaris), Food Chem. 121 (2010) 705–711, https://doi.org/10.1016/j.foodchem.2010.01.009.

[22] M. Dueñas, T. Hernández, I. Estrella, Phenolic composition of the cotyledon and the seed coat of lentils (Lens culinaris L.), Eur. Food Res. Technol. 215 (2002) 478–483, https://doi.org/10.1007/s00217-002-0603-1.

[23] W.M. Mazur, J.A. Duke, K. Wähälä, S. Rasku, H. Adlercreutz, Isoflavonoids and lignans in legumes: nutritional and health aspects in humans, J. Nutr. Biochem. 9 (1998) 193–200, https://doi.org/10.1016/S0955-2863(97)00184-8.

[24] Y. Zou, S.K. Chang, Y. Gu, S.Y. Qian, Antioxidant activity and phenolic compositions of lentil (Lens culinaris var. Morton) extract and its fractions, J. Agric. Food Chem. 59 (2011) 2268–2276, https://doi.org/10.1021/jf104640k.

[25] M.A.-I.E. Faris, H.R. Takruri, A.Y. Issa, Role of lentils (Lens culinaris L.) in human health and nutrition: a review, Mediterr J Nutr Metab 6 (2013) 3–16, https://doi.org/10.1007/s12349-012-0109-8.

[26] A. Troszyńska, I. Estrella, G. Lamparski, T. Hernández, R. Amarowicz, R.B. Pegg, Relationship between the sensory quality of lentil (Lens culinaris) sprouts and their phenolic constituents, Food Res. Int. 44 (2011) 3195–3201, https://doi.org/10.1016/j.foodres.2011.08.007.

[27] M. Świeca, U. Gawlik-Dziki, A. Jakubczyk, Impact of density of breeding on the growth and some nutraceutical properties of ´ready-to-eat lentil (Lens culinaris) sprouts, Acta Sci. Pol. Hortorum Cultus 12 (2013) 19–29.

[28] M. Świeca, B. Baraniak, Influence of elicitation with H_2O_2 on phenolics content, antioxidant potential and nutritional quality of Lens culinaris sprouts, J. Sci. Food Agric. 94 (2014) 489–496, https://doi.org/10.1002/jsfa.6274.

[29] B. Pawlikowska-Pawlega, J. Kapral, A. Gawron, A. Stochmal, J. Zuchowski, Ł. Pecio, R. Luchowski, W. Grudzinski, W.I. Gruszecki, Interaction of a quercetin derivative—Lensoside aβ with liposomal membranes, Biochim. Biophys. Acta Biomembr. 2018 (1860) 292–299, https://doi.org/10.1016/j.bbamem.2017.10.027.

[30] P.I. Oteiza, A.G. Erlejman, S.V. Verstraeten, C.L. Keen, C.G. Fraga, Flavonoidmembrane interactions: a protective role of flavonoids at the membrane surface? Clin. Dev. Immunol. 12 (1) (2005) 19–25, https://doi.org/10.1080/10446670410001722168.

[31] Y.S. Tarahovsky, E.N. Muzafarov, Y.A. Kim, Rafts making and rafts braking: how plant flavonoids may control membrane heterogeneity, Mol. Cell. Biochem. 314 (1–2) (2008) 65–71, https://doi.org/10.1007/s11010-008-9766-9.

[32] S. Selvaraj, S. Krishnaswamy, V. Devashya, S. Sethuraman, U.M. Krishnan, Influence of membrane lipid composition on flavonoid-membrane interactions: implications on their biological activity, Prog. Lipid Res. 58 (2015) (2015) 1–13, https://doi.org/10.1016/j.plipres.2014.11.002.

[33] H. Tsuchiya, Membrane interactions of phytochemicals as their molecular mechanism applicable to the discovery of drug leads from plants, Molecules 20 (2015) 18923–18966, https://doi.org/10.3390/molecules201018923.

[34] A. Maciejczyk, J. Kapral-Piotrowska, J. Sumorek-Wiadro, A. Zając, E. Grela, R. Luchowski, W.I. Gruszecki, M.K. Lemieszek, I. Wertel, Ł. Pecio, J. Żuchowski, K. Skalicka-Woźniak, B. Pawlikowska-Pawlęga, M. Hułas-Stasiak, W. Rzeski, R. Rola, J. Jakubowicz-Gil, Cancers 13 (2021) 2637, https://doi.org/10.3390/cancers13112637.

[35] B. Pawlikowska-Pawlęga, L.E. Misiak, B. Zarzyka, R. Paduch, A. Gawron, W. I. Gruszecki, FTIR, 1H NMR and EPR spectroscopy studies on the interaction of flavone apigenin with dipalmitoylphosphatidylcholine liposomes, Biochim. Biophys. Acta Biomembr. 2013 (1828) 518–527, https://doi.org/10.1016/j.bbamem.2012.10.013.

[36] C.H. Mitchell, D.A. Carre, A.M. McGlinn, R.A. Stone, M.M. Civan, A release mechanism for stored ATP in ocular ciliary epithelial cells, proceedings of the National Academy of science of the United States of, America 95 (1998) (1998) 7174–7178, https://doi.org/10.1073/pnas.95.12.7174.

[37] J. Kapral-Piotrowska, A. Jarosz-Wilkołazka, B. Chudzik, R. Paduch, J. Jakubowicz-Gil, A. Sławińska-Brych, B. Zdzisińska, K. Trębacz, W.I. Gruszecki, B. Pawlikowska-Pawlęga, Apigenin targets protein and lipids of HeLa cells and exhibits protective efficacy against oxidative stress, Acta Pol. Pharm. 80 (1) (2023) 109–127, https://doi.org/10.32383/appdr/163049.

[38] L. Viladevall, R. Serrano, A. Ruiz, G. Domenech, J. Giraldo, A. Barcelo, J. Arino, Characterization of the calcium-mediated response to alkaline stress in Saccharomyces cerevisiae, J. Biol. Chem. 279 (42) (2004) 43614–43624, https://doi.org/10.1074/jbc.M403606200.

[39] L.K. Tamm, S.A. Tatulian, Infrared spectroscopy of proteins and peptides in lipid bilayers, Quartely reviews of, Biophysics 30 (4) (1997) 365–429, https://doi.org/10.1017/s0033583597003375, 1997.

[40] J. Rzymowska, A. Gawron, B. Pawlikowska-Pawlęga, J. Jakubowicz -Gil, J. Wojcierowski, The effect of quercetin on induction of apoptosis, Folia Histochem. Cytobiol. 37 (2) (1999) 125–126.

[41] S.S. Daoud, Cell membranes as targets for anti-cancer drug action, Anti-Cancer Drugs 3 (1992) 443–453, https://doi.org/10.1097/00001813-199210000-00001.

[42] M. Inbar, M. Shinitzky, Cholesterol as a bioregulator in the development and inhibition of leukemia, Proc. Natl. Acad. Sci. USA 71 (1974) 4229–4231, https://doi.org/10.1073/pnas.71.10.4229.

[43] A.B. Hendrich, K. Michalak, Lipids as a target for drugs modulating multidrug resistance of cancer cells, Curr. Drug Targets 4 (1) (2003) 23–30, https://doi.org/10.1016/j.drup.2019.100670.

[44] B. Pawlikowska-Pawlęga, L.E. Misiak, A. Jarosz-Wilkołazka, B. Zarzyka, R. Paduch, A. Gawron, W.I. Gruszecki, Biophysical characterization of genistein–membrane interaction and its correlation with biological effect on cells — the case of EYPC liposomes and human erythrocyte membranes, Biochimica et Biophysica Acta (BBA), Biomembranes 1838 (8) (2014) 2127–2138, https://doi.org/10.1016/j.bbamem.2014.04.029.

[45] B. Pawlikowska-Pawlęga, W.I. Gruszecki, L. Misiak, R. Paduch, T. Piersiak, B. Zarzyka, J. Pawelec, A. Gawron, Modyfication of membranes by quercetin, a naturally occurring flavonoid, via its incorporation in the polar head group, Biochemica et Biophysica Acta 1768 (2007) 2195–2204, https://doi.org/10.1016/j.bbamem.2007.05.027.

[46] V. Ricciardi, M. Portaccio, S. Piccolella, L. Manti, S. Pacifico, M. Lepore, Study of SH-SY5Y Cancer cell response to treatment with polyphenol extracts using FT-IR spectroscopy, Biosensors 7 (2017) 57, https://doi.org/10.3390/bios7040057.

[47] B. Vileno, S. Jeney, A. Sienkiewicz, P.R. Marcoux, L.M. Miller, L. Forró, Evidence of lipid peroxidation andprotein phosphorylation in cells upon oxidative stress photogenerated by fullerols, Biophys. Chem. 152 (2010) 164–169, https://doi.org/10.1016/j.bpc.2010.09.004.

[48] A. Olesko, S. Olsztyńska-Janus, T. Walski, K. Grzeszckuz-Kuc, J. Bujok, K. Galecka, A. Czerski, W. Witkiewicz, M. Komorowska, Application of FTIR-ATR spectroscopy to determinate the extent of lipid peroxidation in plasma during haemodialysis, Biomed. Res. Int. (2015) 245607, https://doi.org/10.1155/2015/245607.

[49] G. Cakmak, I. Togan, C. Uğuz, F. Severcan, FT-IR spectroscopic analysis of rainbow trout liver exposed to Nonylphenol, Appl. Spectrosc. 57 (2003) 835–841, https://doi.org/10.1366/000370203322102933.

[50] A. Derenne, V. Van Hemelryck, D. Lamoral-Theys, R. Kiss, E. Goormaghtigh, FTIR spectroscopy: a new valuable tool to classify the effects of polyphenolic compounds on cancer cells, Biochim. Biophys. Acta 2013 (1832) 46–56, https://doi.org/10.1016/j.bbadis.2012.10.010.

[51] G. Barraza-Garza, H. Castillo-Michel, L.A. De la Rosa, A. Martinez-Martinez, J. A. Pérez-León, M. Cotte, E. Alvarez-Parrilla, Infrared spectroscopy as a tool to study the antioxidant activity of polyphenolic compounds in isolated rat enterocytes, Oxidative Med. Cell. Longev. (2016) 9245150, https://doi.org/10.1155/2016/9245150.

[52] N.P. Ulrih, Analytical techniques for the study of polyphenol–protein interactions, Crit. Rev. Food Sci. Nutr. 57 (2017) 2144–2161, https://doi.org/10.1080/10408398.2015.1052040.

[53] K.Z. Liu, L. Jia, J.S.M. Kelsey, S.M. Newland, A.C. Mantsch, Quantitative determination of apoptosis on leukemia cells by infrared spectroscopy, Apoptosis 6 (2001) 269–278, https://doi.org/10.1023/a:1011383408381.

[54] H.Y. Holman, M.C. Martin, E.A. Blakely, K. Bjornstad, W.R. McKinney, IR spectroscopic characteristics of cell cycle and cell death probed by synchrotron radiation based Fourier transform IR spectroscopy, Biopoly. Biospectrosc. 57 (6) (2000) 329–335, https://doi.org/10.1002/1097-0282(2000)57:6<329::AID-BIP20>3.0.CO;2-2.

[55] F. Gasparri, M. Muzio, Monitoring of apoptosis of HL 60 cells by Fourier-transform infrared spectroscopy, Biochem. J. 369 (2003) 239–248, https://doi.org/10.1042/BJ20021021.

[56] G.A.R. Ahmed, F.A.R. Khorshid, T.A. Kumosani, FT-IR spectroscopy as a tool for identification of apoptosis-induced structural changes in A549 cells treated with PM 701, International Journal of Nano and Biomaterials 2 (2009) 396–408, https://doi.org/10.1504/IJNBM.2009.027736.

[57] N. Elmadany, E. Khail, L. Vaccari, G. Birarda, I. Yousef, R. Abu-Dahab, Antiproliferative activity of the combination of doxorubicin/quercetin on MCF7 breast cancer cell line: a combined study using colorimetric assay and synchrotron infrared microspectroscopy, Infrared Phys. Technol. 95 (2018) (2018) 141–147, https://doi.org/10.1016/j.infrared.2018.10.014.

[58] H.L. Casal, H.H. Mantsch, Polymorphic phase behaviour of phospholipid membranes studied by infrared spectroscopy, Biochem. Biophys. Acta 779 (1984) 381–401, https://doi.org/10.1016/0304-4157(84)90017-0.

[59] H.H. Mantsh, Apoptosis-induced structural changes in leukemia cells identified by IR spectroscopy, J. Mol. 565-566 (2001) 299–304, https://doi.org/10.1016/S0022-2860(00)00817-6.
[60] U. Zelig, J. Kapelushnik, R. Moreh, S. Mordechai, I. Nathan, Diagnosis of cell death by means of infrared spectroscopy, Biophys. J. 97 (7) (2009) 2107–2114, https://doi.org/10.1016/j.bpj.2009.07.026.
[61] B. Pawlikowska-Pawlęga, L.E. Misiak, B. Zarzyka, R. Paduch, A. Gawron, W. I. Gruszecki, Localization and interaction of genistein with model membranes formed with dipalmitoylphosphatidylcholine (DPPC), Biochim. Biophys. Acta Biomembr. 2012 (1818) 1785–1793, https://doi.org/10.1016/j.bbamem.2012.03.020.
[62] B. Pawlikowska-Pawlęga, H. Dziubińska, E. Król, K. Trębacz, A. Jarosz-Wilkołazka, R. Paduch, A. Gawron, W.I. Gruszecki, Characteristics of quercetin interactions with liposomal and vacuolar membranes, Biochim. Biophys. Acta Biomembr. 1838 (2014) 254–265, https://doi.org/10.1016/j.bbamem.2013.08.014.
[63] B. Bellisola, C. Sorio, Infrared spectroscopy and microscopy in cancer research and diagnosis, Am. J. Cancer Res. 2 (1) (2012) 1–21.
[64] S. Machana, N. Weerapreeyakul, S. Barusrux, K. Thumanu, W. Tanthanuch, Synergistic anticancer effect of the extracts from Polyalthia evecta caused apoptosis in human hepatoma (HepG2) cells, Asian Pac. J. Trop. Biomed. 2 (8) (2012) 589–596, https://doi.org/10.1016/S2221-1691(12)60103-8.
[65] F.A. Khorshid, The cytotoxic effect of PM 701 and its fractions on cell proliferation of breast Cancer cells, MCF7, American journal of, Drug Discovery and Development 1 (2011) 200–208, https://doi.org/10.3923/ajdd.2011.200.208.
[66] Y. Gao, X. Huo, L. Dong, X. Sun, H. Sai, G. Wei, Y. Xu, Y. Zhang, J. Wu, Fourier transform infrared microspectroscopy monitoring of 5-fluorouracil-induced apoptosis in SW620 colon cancer cells, Mol. Med. Rep. 11 (4) (2014) 2585–2591, https://doi.org/10.3892/mmr.2014.3088.
[67] M. Yoshida, T. Sakai, N. Hosokawa, N. Marui, K. Matsumoto, A. Fujioka, H. Nishino, A. Aoike, The effect of quercetin on cell cycle progression and growth of human gastric cancer cells, FEBS Lett. 260 (1) (1990) 10–13, https://doi.org/10.1016/0014-5793(90)80053-l.
[68] J.A. Choi, J.Y. Kim, J.Y. Lee, C.M. Kang, H.J. Kwon, Y.D. Yoo, T.W. Kim, Y.S. Lee, S.J. Lee, Induction of cell cycle arrest and apoptosis in human breast cancer cells by quercetin, Int. J. Oncol. 19 (4) (2001) 837–844, https://doi.org/10.3892/ijo.19.4.837.
[69] M. Richter, R. Ebermann, B. Marian, Quercetin-induced apoptosis in colorectal tumor cells: possible role of EGF receptor signaling, Nutr. Cancer 34 (1) (1999) 88–99, https://doi.org/10.1207/S15327914NC340113.
[70] T.M. El Attar, A.S. Virji, Modulating effect of resveratrol and quercetin on oral cancer cell growth and proliferation, Anti-Cancer Drugs 10 (2) (1999) 187–193, https://doi.org/10.1097/00001813-199902000-00007.
[71] G. Wang, J. Zhang, L. Liu, S. Sharma, Q. Dong, Quercetin potentiates doxorubicin mediated antitumor effects against liver cancer through p53/Bcl-xl, PLoS One 7 (12) (2012) e51764, https://doi.org/10.1371/journal.pone.0051764.
[72] H.K. Nair, K.V. Rao, R. Aalinkeel, S. Mahajan, R. Chawda, S.A. Schwartz, Inhibition of prostate cancer cell colony formation by the flavonoid quercetin correlates with modulation of specific regulatory genes, Clin. Diagn. Lab. Immunol. 11 (1) (2004) 63–69, https://doi.org/10.1128/cdli.11.1.63-69.2004.
[73] E. Mutlu Altundağ, T. Kasacı, A.M. Yılmaz, B. Karademir, S. Koçtürk, Y. Taga, A. S. Yalçın, Quercetin-induced cell death in human papillary thyroid cancer (B-CPAP) cells, J. Thyroid. Res. (2016) 9843675, https://doi.org/10.1155/2016/9843675.
[74] T.J. Lee, O.H. Kim, Y.H. Kim, J.H. Lim, S. Kim, J.W. Park, T.K. Kwon, Quercetin arrests G2/M phase and induces caspase-dependent cell death in U937 cells, Cancer Lett. 240 (2) (2006) 234–242, https://doi.org/10.1016/j.canlet.2005.09.013.
[75] E. Angst, J.L. Park, A. Moro, Q.Y. Lu, X. Lu, G. Li, J. King, M. Chen, H.A. Reber, V.L. W. Go, The flavonoid quercetin inhibits pancreatic cancer growth in vitro and in vivo, Pancreas 42 (2) (2013) 223, https://doi.org/10.1097/MPA.0b013e318264ccae.
[76] SY. Zheng, Y. Li, D. Jiang, J. Zhao, J.F. Ge, 2012, anticancer effect and apoptosis induction by quercetin in the human lung cancer cell line A-549, Mol. Med. Rep. 5 (3) (2012) 822–826. doi:https://doi.org/10.3892/mmr.2011.726.
[77] A.F. Clemente-Soto, E. Salas-Vidal, C. Milan-Pacheco, J.N. Sanchez- Carranza, O. Peralta-Zaragoza, L. Gonzalez-Maya, Quercetin induces G2 phase arrest and apoptosis with the activation of p53 in an E6 expression-independent manner in HPV-positive human cervical cancer-derived cells, Mol. Med. Rep. 19 (3) (2019) 2097–2106, https://doi.org/10.3892/mmr.2019.985015.
[78] M. Kedhari Sundaram, A. Hussain, S. Haque, R. Raina, N. Afroze, Quercetin modifies 5′CpG promoter methylation and reactivates various tumor suppressor genes by modulating epigenetic marks in human cervical cancer cells, J. Cell. Biochem. 120 (10) (2019) 18357–18369, https://doi.org/10.1002/jcb.2914716.
[79] M. Kedhari Sundaram, A. Raina, N. Afroze, K. Bajbouj, M. Hamad, S. Haque, A. Hussain, Quercetin modulates signaling pathways and induces apoptosis in cervical cancer cells, Biosci Rep. 2019 39 (8) (2019), https://doi.org/10.1042/BSR20190720. BSR20190720.
[80] W. Zhang W, X.U. Xiaoxial, H. Chen, J. Zhang, X. Zhang, R. Luo, F. Fang, Effect of quercetin on breeding and apoptosis of cervical Cancer 85 HeLa cell and on growth of transplanted tumor in nude mice, Wuhan University Journal of Natural Sciences 12 (3) (2007) 569–576, https://doi.org/10.1007/s11859-006-0120-3.
[81] W.H. Talib, M.H. Abu Zarga, A.M. Mahasneh, Antiproliferative, antimicrobial and apoptosis inducing effects of compounds isolated from *Inula viscosa*, Molecules 17 (2012) 3291–3303, https://doi.org/10.3390/molecules17033291.
[82] S. Wang, Q. Tian, F. An, Growth inhibition and apoptotic effects of total flavonoids from Trollius chinensis on human breast cancer MCF-7 cells, Oncol. Lett. 12 (2016) (2016) 1705–1710, https://doi.org/10.3892/ol.2016.4898.
[83] V.R. Priyadarsini, S.R. Murugan, S. Maitreyi, K. Ramalingam, D. Karunagaran, S. Nagini, The flavonoid quercetin induces cell cycle arrest and mitochondria-mediated apoptosis in human cervical cancer (HeLa) cells through p53 induction and NF-κB inhibition, Eur. J. Pharmacol. 649 (2010) 84–91, https://doi.org/10.1177/0960327109107002.
[84] G. Ferrandina, G. Almadori, N. Maggiano, P. Lanza, C. Ferlini, P. Cattani, M. Piantelli, G. Scambia, F.O. Ranelletti, Growth-inhibitory effect of tamoxifen and quercetin and presence of type ii estrogen binding sites in human laryngeal cancer cell lines and primary laryngeal tumors, Int. J. Cancer 77 (1998) (1998) 747–754, https://doi.org/10.1002/(sici)1097-0215(19980831)77:5<747::aid-ijc14>3.0.co;2-z.
[85] S. Ranganathan, D. Halagowder, N.D. Sivasithambaram, Quercetin suppresses twist to induce apoptosis in MCF-7 breast Cancer cells, PLoS One 10 (10) (2015) e0141370, https://doi.org/10.1371/journal.pone.0141370.
[86] V. Helfinger, K. Schroder, Redox control in cancer development and progression, Mol. Asp. Med. 63 (2018) 88–98, https://doi.org/10.1016/j.mam.2018.02.003.
[87] S. Habtemarium, E. Dagne, Comparative antioxidant, prooxidant and cytotoxic activity of sigmoidin a and eriodictyol, Planta Med. 76 (2010) 589–594, https://doi.org/10.1055/s-0029-1240604.
[88] N. Li, J.H. Liu, J. Zhang, B.Y. Yu, Comparative evaluation of cytotoxicity and antioxidative activity of 20 flavonoids, J. Agric. Food Chem. 56 (2008) 3876–3883, https://doi.org/10.1021/jf073520n.
[89] L. Gibellini, M. Pinti, M. Nasi, S. De Biasi, E. Roat, L. Bertoncelli, A. Cossarizza, Interfering with ROS metabolism in Cancer cells: the potential role of quercetin, Cancers (Basel) 2 (2) (2010) 1288–1311, https://doi.org/10.3390/cancers2021288.
[90] K. Bishayee, S. Ghosh, A. Mukherjee, R. Sadhukhan, J. Mondal, A.R. Khuda-Bukhsh, Quercetin induces cytochrome-C release and ROS accumulation to promote apoptosis and arrest the cell cycle in G2/M, in cervical carcinoma: signal Cascade and drug-DNA interaction, Cell Prolif. 46 (2013) 153–163, https://doi.org/10.1111/cpr.12017.
[91] Y.F. Chang, Y.C. Hsu, H.F. Hung, H.J. Lee, W.Y. Lui, C.W. Chi, J.J. Wang, Quercetin induces oxidative stress and potentiates the apoptotic action of 2-Methoxyestradiol in human hepatoma cells, Nutr. Cancer 61 (5) (2009) 735–745, https://doi.org/10.1080/01635580902825571.
[92] K.C. Liu, C.Y. Yen, R.S. Wu, J.S. Yang, H.F. Lu, K.W. Lu, C. Lo, H.Y. Chen, N. Y. Tang, C.C. Wu, J.G. Chung, The roles of endoplasmic reticulum stress and mitochondrial apoptotic signaling pathway in quercetin-mediated cell death of human prostate cancer PC-3 cells, Environ. Toxicol. 29 (4) (2014) 428–439, https://doi.org/10.1002/tox.21769.
[93] X. Zhang, J. Huang, C. Yu, L. Xiang, L. Li, D. Shi, F. Lin, Quercetin enhanced paclitaxel therapeutic effects towards PC-3 prostate cancer through ER stress induction and ROS production, Onco Targets Ther 13 (2020) 513–523, https://doi.org/10.2147/OTT.S228453.
[94] H.S. Shang, H.F. Lu, C.H. Lee, H.S. Chiang, Y.L. Chu, A. Chen, Y.F. Lin, J.G. Chung, Quercetin induced cell apoptosis and altered gene expression in AGS human gastric cancer cells, Environ. Toxicol. 33 (11) (2018) 1168–1181, https://doi.org/10.3892/ijmm.2016.2625.
[95] Y. Zhang, Y. Guo, M. Wang, H. Dong, J. Zhang, L. Zhang, Quercetrin from Toona sinensis leaves induces cell cycle arrest and apoptosis via enhancement of oxidative stress in human colorectal cancer SW620 cells, Oncol. Rep. 38 (6) (2017) 3319–3326, https://doi.org/10.3892/or.2017.6042.
[96] A.J. Vargas, R. Burd, Hormesis and synergy: pathways and mechanisms of quercetin in cancer prevention and management, Nutr. Rev. 68 (7) (2010) 418–428, https://doi.org/10.1111/j.1753-4887.2010.00301.x.